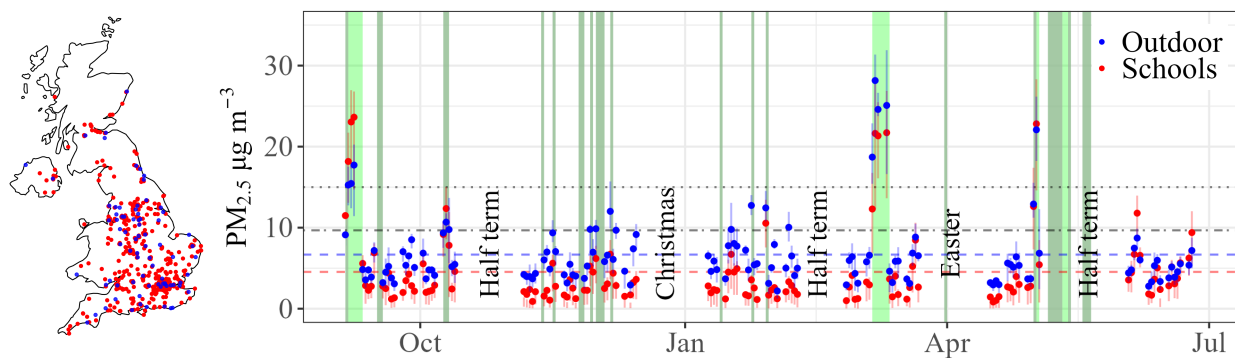


Graphical Abstract

Particulate matter concentrations in UK schools: a nationwide study into the influence of ambient $\text{PM}_{2.5}$ and the resulting exposure potentials

Alice E. E. Handy, Samuel G. A. Wood, Katherine Roberts, Christopher S. Malley, Henry C. Burridge, The SAMHE Project Consortium



Highlights

Particulate matter concentrations in UK schools: a nationwide study into the influence of ambient PM_{2.5} and the resulting exposure potentials

Alice E. E. Handy, Samuel G. A. Wood, Katherine Roberts, Christopher S. Malley, Henry C. Burridge, The SAMHE Project Consortium

- Concentrations of PM_{2.5} were monitored in 490 schools across the UK during the academic year 2023–2024.
- School PM_{2.5} concentrations closely correlated to ambient outdoor PM_{2.5} concentrations.
- Outdoor air is a key source of PM_{2.5} in the schools monitored, an upper bound for the contribution from indoor sources is estimated to be 25%.
- Outdoor PM_{2.5} events — periods of elevated outdoor PM_{2.5} concentration — lead to high concentrations in schools.
- The potential exposure of PM_{2.5} received during these PM_{2.5} events is estimated to contribute significantly to the potential total exposure over the academic year.

Particulate matter concentrations in UK schools: a nationwide study into the influence of ambient PM_{2.5} and the resulting exposure potentials

Alice E. E. Handy^{a,1,*}, Samuel G. A. Wood^a, Katherine Roberts^a, Christopher S. Malley^b, Henry C. Burridge^a, The SAMHE Project Consortium

^a*Department of Civil and Environmental Engineering, Imperial College London, London, SW7 2AZ, UK*

^b*Stockholm Environment Institute, Environment Building, Wentworth Way, University of York, York, YO10 5NG, UK*

Abstract

This paper analyses the concentration of particulate matter PM_{2.5} from monitors deployed, by the Schools' Air Quality Monitoring for Health and Education Initiative (SAMHE), to 490 schools across the United Kingdom throughout the academic year 2023—2024. The data shows that the PM_{2.5} concentration in schools is closely correlated to the ambient outdoor PM_{2.5} concentrations. Whilst the evidence gathered indicates that sources of PM_{2.5} within schools contribute to the concentrations, it is shown that outdoor sources are the dominant signature within the PM_{2.5} concentration measurements made indoors. Moreover, over the academic year, outdoor PM_{2.5} events — periods of elevated outdoor PM_{2.5} concentration — are shown to account for approximately 41% of the total potential exposure, whilst occurring on only around 13% of schooldays. These, and other findings presented herein, have important implications for school air quality and how air quality within schools, and beyond, is managed.

Keywords: Particulate Matter, PM_{2.5}, Schools' Air Quality, Exposure, UK, Indoor, Outdoor

1. Introduction

The detrimental effects of particulate matter (PM) on health are well documented and are linked to adverse respiratory and cardiovascular health effects (Kim et al., 2015). Particular attention is given to the harmful effects of particulate matter with an aerodynamic diameter less than 2.5 μm (PM_{2.5}) as these fine particles can penetrate deeper into the lung, with a proportion of ultrafine particles (PM_{0.1}) crossing over into the bloodstream to reach other organs (Exley et al., 2022). Children are more vulnerable to the detrimental effects of PM_{2.5} as they breathe in a larger amount of air per unit body mass compared to adults, which can have damaging effects on their developing immune systems and lungs (Rees, 2017). Long-term exposure to PM_{2.5} is associated with negative effects on lung development and with the exacerbation of asthma in children (Son, 2023; Exley et al., 2022). This can result in increased school absenteeism, an increased need for doctor visits, hospitalisation and is detrimental to children's well-being (Zhang et al., 2022). Beyond the consequences on children's health, poor air quality is linked to a reduction in cognitive performance which can have negative consequences for pupil attainment (Wargocki et al., 2020; Sadrizadeh et al., 2022).

School buildings are a key environment for children where they spend approximately 30% of their time (Son, 2023; Faria et al., 2020). It is therefore essential to measure and understand the concentrations of PM_{2.5} in schools. Clearly, providing a safe and healthy environment for children is essential, and whilst there are no guidelines specific to particulate matter in UK schools, the World Health Organisation recommends that, on health-based grounds, the 24-hour mean concentration of PM_{2.5} of both indoor and outdoor air should not exceed 15 $\mu\text{g}/\text{m}^3$ (WHO, 2021).

*Corresponding author

¹*E-mail address:* a.handy23@imperial.ac.uk

Particulate matter in schools can originate from indoor sources or outdoor sources brought inside through openings in the building fabric (e.g. windows and doors) — it is an aim of this study to contribute findings on the relative importance of indoor and outdoor sources for the $\text{PM}_{2.5}$ concentrations measured in schools. Many studies have shown that school occupants, resuspension of settled dust, and outdoor air are significant contributing sources of particulate matter in school classrooms (Amato et al., 2014; Faria et al., 2020; Becerra et al., 2020). For example, Amato et al. (2014) collected $\text{PM}_{2.5}$ samples from indoor and outdoor environments of 39 primary schools and found 47% of indoor samples to have originated from indoor sources (including skin flakes, clothes fibres, VOC’s, and the resuspension of soil particles) and the remaining 53% of indoor sources to have infiltrated into the classroom from outdoors. The indoor-outdoor ratio of particulate matter within schools can vary significantly depending on building design, building operation, ventilation, and the intensity of outdoor pollution sources (Poupard et al., 2005; Stamp et al., 2022; Mohammadyan et al., 2017). Particulate matter in the outdoor air that surrounds school buildings can originate from sources generated locally (such as roadside traffic pollution and road dust), as well as regional sources like industrial emissions, and even trans-boundary sources (Mohammadyan et al., 2017; Harrison et al., 2012).

Studies that have investigated $\text{PM}_{2.5}$ in schools predominantly consider cohorts of schools within a specific urban setting or region, are often limited in the number of schools they include, and are short-term in their nature. It is therefore challenging to extrapolate findings to implications for the national school stock (in the UK approximately 23 000 schools). The SAMHE method allows for longitudinal monitoring of $\text{PM}_{2.5}$ concentrations, amongst other indoor air quality (IAQ) metrics, in schools across the UK. In this paper, we consider a national dataset of concentration of $\text{PM}_{2.5}$ in 490 schools at locations across the UK over the academic year 2023—2024.

This paper investigates the temporal trends in school $\text{PM}_{2.5}$ concentrations across an entire academic year. Attention is given not only to the long-term impact of $\text{PM}_{2.5}$ in schools through evaluation of a ‘potential exposure’, but also to episodes of elevated PM concentration, or ‘ $\text{PM}_{2.5}$ events’, which can have pertinent consequences for acute health. The remainder of this paper is structured as follows. The details of the SAMHE methodology which facilitates the collection of a large longitudinal dataset is outlined in §2.1. The formation of the $\text{PM}_{2.5}$ concentration datasets analysed in this paper is described in §2.2.1 and §2.2.2 for the SAMHE schools and outdoor $\text{PM}_{2.5}$ concentration respectively. In §3, the results of this study are presented, beginning with examining the $\text{PM}_{2.5}$ concentration trends over the academic year in §3.1. The impact of ‘outdoor $\text{PM}_{2.5}$ events’ on the concentration in schools is then evaluated in §3.2, and in §3.3 it is shown that these events contribute significantly to the total potential exposure of $\text{PM}_{2.5}$ received at school over the academic year. Finally, in §4 conclusions are drawn.

2. Methods

2.1. SAMHE methodology

This paper analyses indoor air quality data from within the 490 UK schools that sent data as part of the SAMHE project during the academic year 2023-2024, herein 05/Sep/23–25/Jun/24. Through a standardised method (documented by Chatzidiakou et al., 2023; West et al., 2023) the SAMHE project, as part of the SAMHE initiative, has begun gathering a longitudinal dataset of indoor air quality in school throughout the UK. During the recruitment phase of the project (May 2023 to May 2024) any UK school (providing education to pupils aged above four years old) could apply to participate in SAMHE. Recruitment efforts were made to ensure that participating schools represented the UK school population in certain key demographics, including fee-paying versus state-funded schools, their constituent country within the UK, and Index of Multiple Deprivation (IMD, which ranks areas based on several metrics of relative deprivation). Once a school was accepted as a SAMHE school, they were sent a free WiFi-enabled low-cost air quality monitor and provided with instructions on how to connect it to their school’s internet network and where to place the monitor within classrooms to be approximately at head height and not near windows or external walls. The remote approach of this methodology leads to the location of monitors within schools not being recorded by the researchers, however, given the size of the dataset in this study, it is likely that the majority of measurements are taken within classrooms. Each school was also provided with ongoing access to a

Web-App, where the air quality data recorded by their SAMHE monitor can be visualised and, through which, tailor-made curriculum-linked resources are made available. As of September 2024, 882 SAMHE monitors within schools had recorded IAQ data, 490 of which met data completeness criteria to be analysed within this paper. During the study period, SAMHE monitors record readings every minute of: CO₂, relative humidity, total volatile organic compounds, temperature, and particulate matter; the last of which is ultimately measured via a ‘Plantower PMS5003’ sensor (which employs a laser scattering principle) — these PM_{2.5} measurements form the focus of this study.

2.2. Description of the datasets

2.2.1. Data from the SAMHE dataset

This study analyses a subset of all the concentrations of PM_{2.5} recorded by SAMHE schools’ monitors, over the period from the start of the Autumn term 2023 to the end of Summer term 2024. We consider the school-year to start on the first day that all UK schools are expected to be ‘in term’ during the autumn of 2023 and finish on the last day that all UK schools are expected to be ‘in term’ during the summer 2024. Within this period we define non-school days to include: weekends, any days on which schools within the four nations of the UK are out of term-time and on ‘school holidays’, and any days which are local or national holidays within any UK nation. As such, on any schoolday all SAMHE schools are expected to be active (i.e. have pupils in attendance). The dates on which SAMHE schools are deemed to be ‘in term’ are summarised, by each ‘half-term’, in table A.1.

We consider two periods of time and, for each, two associated datasets. First, we describe the 24-hour period every day (including non-school days, e.g. weekends, etc.) from the start of the Autumn term 2023 to end of Summer term 2024 as the “continuous period” — a period of 295 days in total — and the analysis of the PM_{2.5} concentrations throughout this period as being analysis of the “continuous period dataset”. Second, the “school-year” describes only every schoolday and only between the hours of 09:00 and 16:00 (the occupied period (HM Government, UK, 2018)) — 133 days in total — and the analysis of the PM_{2.5} concentrations throughout the school-year being the analysis of the “schoolday dataset”. The processes of forming the datasets are described below and are summarised in the flow diagram of figure B.1.

On each day of the continuous period, data is only included from schools that report minutely PM_{2.5} concentrations for more than 75% of the 24-hours, i.e. for more than 1080 minutes, following protocols used by EPA (Duvall et al., 2021). During the academic year 2023–2024, the SAMHE project recruited an increasing number of schools. As a consequence, the number of schools from which data can be included within this study increased throughout the year. On all days, and for each school, a mean over the full 24-hour period is calculated; the average of these values over the included schools are described as the “SAMHE 24-hour mean PM_{2.5} concentration”, providing a dataset of 295 values. The minimum number of schools reporting data that met the inclusion criteria on any day within the continuous period dataset was 123 and the maximum was 339; as such, the ‘SAMHE 24-hour mean PM_{2.5} concentrations’ reported herein for each day always reflect averages across between 123 and 339 schools.

The ‘schoolday dataset’ is formed by, on each schoolday, selecting only the schools that report PM_{2.5} concentrations for more than 75% of the time during the school day, i.e. for more than 315 minutes between 09:00 and 16:00. On all schooldays, and for each school, a mean over the duration between 09:00 and 16:00 is calculated; the average of these values over the included schools are described as the “SAMHE schoolday mean PM_{2.5} concentration”, providing a dataset of 133 values. It is natural that, on a given day, there are more schools that meet the data completeness criteria during the 7 hours of the schoolday period than those meeting the data completeness criteria over the 24-hour period. For the schoolday dataset, the minimum number of included schools on any schoolday was 136 and maximum was 346; as such, the ‘SAMHE schoolday mean PM_{2.5} concentrations’ reported herein for each day always reflect averages across between 136 schools and 346 schools.

In total over the year, this study reports on data gathered from within 490 schools across the UK (see figure 1 for an illustration of their locations). Herein, the analysis will be evaluating the 24-hour mean PM_{2.5} concentrations and schoolday mean PM_{2.5} concentrations — as shown in Appendix C, the probability density distributions of concentrations are largely unchanged between the primary datasets reported in §3 (i.e. taking 1-day means) and either examining the minutely data or taking hourly means.

The extent to which the results of this study are sensitive to the data completeness criteria, and the construction of the datasets analysed, is evaluated by comparing the results based on analysis of the primary datasets (presented in §3) to those that would be deduced should alternate datasets, resulting from a different construction, be analysed. The alternate datasets are constructed by, in addition to the above completeness criteria, insisting that each included school also meets these inclusion criteria on more than 75% of schooldays within the school-year (i.e. on more than 99 schooldays). Hence, whilst the population of schools included within the primary datasets can evolve as schools join SAMHE and schools’ monitors become connected, disconnected, or reconnected, the population of included schools within the alternate datasets remains fixed over the entire academic year. Comparing summary statistics of the primary and alternate datasets, see [Appendix D](#), illustrates that the findings and conclusions of this study remain unchanged irrespective of the choice of dataset construction made.

2.2.2. Other datasets

The SAMHE $PM_{2.5}$ concentration datasets are compared in §3 to datasets constructed from measurements of ambient outdoor $PM_{2.5}$ concentrations based on those reported by Defra AURN monitoring sites, and only those recorded at sites being representative of ambient ‘background’ levels. These concentrations of $PM_{2.5}$ are reported at hourly intervals by the AURN sites, and we identify the nearest background AURN site to each included SAMHE school — only data from these sites are used in the analysis presented. We constrain our analysis to ‘background’ AURN sites which are intended to be the sites positioned so that the pollution data recorded is representative of several square kilometres and not influenced by any single local source of pollution (see [Defra AURN, 2024](#)). Industrial and traffic sites are omitted since these are positioned to capture the effects of pollution due to specific industrial activities or nearby traffic which, it is expected, is less representative of the outdoor air quality surrounding SAMHE school buildings.

The number of AURN sites from which data is selected can vary each day depending on the SAMHE schools included in the datasets on that day, and is further affected by the completeness of data reported by AURN sites, see [figure B.1](#) for an overview of the formation of the datasets. An equivalent data completeness criteria was applied to the data from AURN sites to that of the SAMHE schools. That is, for the continuous period, on each day only sites that reported concentrations of $PM_{2.5}$ data for more than 75% of the 24-hours were included. On each day, out of these sites, the AURN site nearest to each included school (included within the ‘continuous period SAMHE dataset’ on that day) is selected — based upon the geographical distance — with some AURN sites being the nearest to many schools. The analysis of the “continuous period AURN dataset” describes the analysis of the 295 “AURN 24-hour mean $PM_{2.5}$ concentrations” which are calculated for each day within the continuous period as the average of the 24-hour mean $PM_{2.5}$ concentrations from each included AURN site, on each day. Over the continuous period, the minimum number of AURN sites from which data is included, on any given day, to calculate the ‘AURN 24-hour mean $PM_{2.5}$ concentration’ is 49, and maximum is 66. The mean of the distances between each school and the nearest AURN site varies each day between 14.2km and 18.3kmas each day the selected schools and nearest AURN site to each vary depending on the adherence to the data completeness criteria..

Similarly, to form the “school-year AURN dataset”, only AURN sites that report data for more than 75% of a given schoolday, between the duration 09:00-16:00, are included for that day. Each schoolday, from these sites, the nearest site to each included school in the school-year SAMHE dataset is found. Then, for each AURN site, a mean $PM_{2.5}$ concentration over each schoolday (between 09:00 and 16:00) is calculated, these values, averaged across all included sites are described as the “AURN schoolday mean $PM_{2.5}$ concentrations” — providing another dataset of 133 values. The minimum number of AURN sites included in the ‘school-year AURN dataset’, on any given day, is 50, and the maximum is 67. The mean of the distances between each school and the nearest AURN site varies each schoolday between 14.8 km and 19.2 km. Over the year, data from 77 AURN sites in total were used in this study, the locations of these are shown in [figure 1](#).

As will be revealed in §3, high concentrations of $PM_{2.5}$ were recorded in SAMHE schools when the outdoor concentration measurements were elevated — to aid analysis we categorise periods of elevated outdoor $PM_{2.5}$ concentrations as ‘ $PM_{2.5}$ events’. Two sets of outdoor $PM_{2.5}$ events are defined as any day, or set of consecutive days, when the AURN 24-hour mean $PM_{2.5}$ concentration exceeds a threshold value

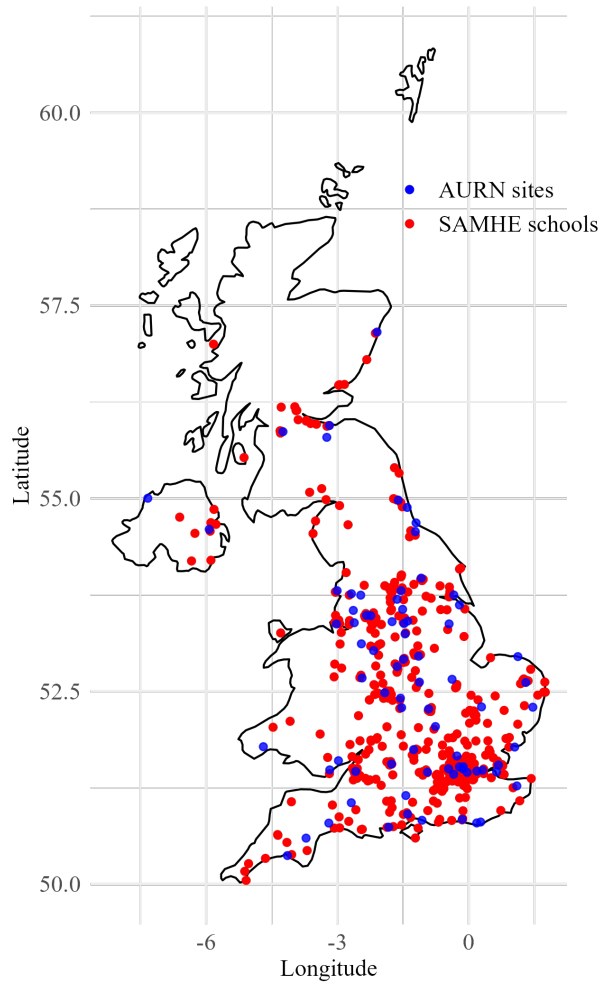


Figure 1: Map outlining the UK (i.e. Great Britain and Northern Ireland), showing the location of the schools from which data is included in the reported analysis, and the location of the background AURN sites used within the analysis (that are those nearest to the schools).

of $15 \mu\text{g}/\text{m}^3$ (as per WHO guidance (WHO, 2021)), or a threshold defined as the median plus one standard deviation of the measured data (see §3.2).

2.3. Error analysis for large-scale datasets from low-cost monitors

Carrying out meaningful co-location tests for all the SAMHE monitors which sent data from within 490 schools around the UK was not feasible, nor would it be a reasonable use of resources. Co-location tests have been carried out using AirGradient monitors (as used by SAMHE) at four different sites around the UK. At three of those sites, all monitors were exposed to outdoor air, whilst in the fourth all the monitors were placed indoors. At each site, multiple AirGradient monitors, which employ ‘low-cost’ Plantower PMS5003 sensors within them, were co-located with a gravimetric, or high-accuracy, particulate matter monitor (these were reference grade devices at all of the outdoor sites AirGradient, 2024). These tests provided co-located data consisting of 3,246 and 384 independent observations of the daily mean concentrations at the outdoor sites and indoor site, respectively; see table G.1 for details of the tests.

The root mean square error (RMSE) between all observations of daily mean concentration by the low-cost Plantower PMS5003 sensors, relative to their co-located monitors, was $2.45 \mu\text{g}/\text{m}^3$, with the mean absolute error being $1.87 \mu\text{g}/\text{m}^3$. Examining the data from any one of the four sites individually provides reassuringly consistent estimates of the errors, see appendix Appendix G for full details. Similar analysis cannot be replicated for the SAMHE monitors directly since they reside within the 490 schools across the UK. A metric which can be calculated for both the Plantower PMS5003 sensors within the co-located, and the SAMHE, datasets is the estimate of standard error — the mean values (with the lower and upper quartiles included in square brackets) of these are $0.27 \mu\text{g}/\text{m}^3$ [$0.22 \mu\text{g}/\text{m}^3$, $0.32 \mu\text{g}/\text{m}^3$] for the SAMHE dataset and $0.38 \mu\text{g}/\text{m}^3$ [$0.18 \mu\text{g}/\text{m}^3$, $0.80 \mu\text{g}/\text{m}^3$] for those co-located. The consistency in the values obtained from the two dataset between provides some confidence that errors within the co-located dataset are representative of the errors with the measurements from the SAMHE monitors.

Finally, we note that all estimates of errors from the measurements by Plantower PMS5003 PM sensors analysed (e.g. RMSE of $2.45 \mu\text{g}/\text{m}^3$ and MAE of $1.87 \mu\text{g}/\text{m}^3$ from the co-located dataset, noting that these measures reflect both systematic and random errors) are small relative to the natural variations in SAMHE measurements being analysed herein. For example, the standard deviation in daily mean values is $4.80 \mu\text{g}/\text{m}^3$ over the school year, and $3.68 \mu\text{g}/\text{m}^3$ over the continuous period. A Levene’s test confirms that the variance associated with these errors of Plantower PMS5003 measurement i.e. the mean square errors, are small relative to the variance of the SAMHE datasets ($F(1, 3380) = 74.72$, with a p-value $p < 2.2 \times 10^{-16}$ for the school year data and $F(1, 3535) = 52.97$, with a p-value $p = 4.15 \times 10^{-16}$ for the continuous period). Thus, estimates of the errors associated with the measurements of low-cost sensors $\text{PM}_{2.5}$ sensors deployed within the SAMHE Initiative are sufficiently small to warrant the analysis presented (§3) and the conclusions drawn.

For completeness, we desired to calculate all of our results based on both the raw measurements gathered by the Plantower PMS5003 PM sensors within the SAMHE monitors (§3), and for an adjusted dataset which factors in the results from co-located data tests (Appendix H). To do so, we took the measurements from the co-location dataset and calculate a regression to provide a linear mapping of the daily mean concentrations measured by the low-cost PMS5003 sensors to best-fit their co-located monitors. This linear mapping was then utilised to create ‘adjusted SAMHE datasets’. Analysis of the unadjusted ‘primary SAMHE datasets’ are reported throughout §3, and we quantify details of all changes when the adjusted SAMHE datasets in Appendix H — crucially, all of our findings and conclusions remain unchanged.

3. Results

Over the academic year the SAMHE $\text{PM}_{2.5}$ concentrations vary considerably, see figure 2. Moreover, there is often a larger variation in SAMHE $\text{PM}_{2.5}$ concentrations per day than between schools, as shown in figures 2a and 2b by a greater difference between values of the red circular markers than the height of the vertical red bars which show the interquartile range of daily-mean values measured across included

SAMHE schools. The SAMHE $\text{PM}_{2.5}$ concentration when considering just the period that schools are occupied (between 09:00-16:00 on schooldays) is typically higher than the SAMHE 24-hour mean $\text{PM}_{2.5}$ concentrations on a given day. Over the entire year, the mean of the SAMHE schoolday dataset, i.e. the mean of the 133 values of SAMHE schoolday mean $\text{PM}_{2.5}$ concentrations, is $4.54 \mu\text{g}/\text{m}^3$, where the tolerance indicated the standard deviation.. This is higher than the associated mean of the continuous period dataset, i.e. the mean of the 295 SAMHE 24-hour $\text{PM}_{2.5}$ concentrations, of $3.71 \mu\text{g}/\text{m}^3$. These mean values are indicated by the red dashed lines in figures 2a and 2b, and the mean, median and standard deviation of both the continuous period and schoolday datasets are given in the first row of table C.1. It is, however, worth noting that the mean measurements are both small compared to the extreme variations; for example, for both the continuous period and schoolday datasets the differences between the maximum and minimum of the daily values obtained are over $20 \mu\text{g}/\text{m}^3$. The indoor-outdoor ratio, as shown in figure 2c, is typically less than unity in value, however, is also highly variable. When comparing the continuous period dataset, i.e. ratios associated with 24-hour means shown by grey markers, to the schoolday dataset, the ratios associated with on the 09:00-16:00 means only on schooldays shown by purple markers, the ratio is typically higher for the schoolday dataset.

We note that the mean $\text{PM}_{2.5}$ concentrations measured in SAMHE schools over the year are within the range of some studies published in the literature, and lower than others (e.g. Hama et al., 2023; European Commission et al., 2014). A systematic review (Son, 2023) has shown that concentrations in classrooms varied widely, and varied between nations — they did not include UK schools, but we note that from the studies they did review from within 8 nations, the concentrations were reported in the range of 8–100 $\mu\text{g}/\text{m}^3$. Furthermore, some of the studies reviewed therein selected schools which were deliberately near to a particular pollution source; for example, the study that reported the highest value (100 $\mu\text{g}/\text{m}^3$), investigated the impact of the school’s wood-burning heating system on air quality. None of these studies continually monitored any schools for an entire academic year, most frequently sampling for a period of one to two weeks. These studies we conducted as early as 1997 and as recently as 2013. We note that the annual mean ambient outdoor concentration of $\text{PM}_{2.5}$ fell by $4.8 \mu\text{g}/\text{m}^3$ between 2013 and 2023 in the UK (DEFRA, 2024) with similar reductions in Europe (EEA, 2013, 2024). Nevertheless, we note that most studies reviewed therein deployed gravimetric sampling whilst the $\text{PM}_{2.5}$ sensors for SAMHE monitors use a laser scattering principle (see §2.1). However, the errors associated with using low-cost laser scattering sensors have been estimated to be small compared to the variance of daily mean concentrations in the SAMHE dataset, see §2.3. Crucially, the primary focus of the present study is the relative changes in concentration due to the changes in outdoor concentration; in what follows, the data gathered by the SAMHE monitors is compared to (outdoor) measurements from reference grade gravimetric measurement stations installed and maintained by the UK government — the comparison shows reassuring patterns and reasonable values for indoor-outdoor ratios.

To contextualise the large variation in $\text{PM}_{2.5}$ concentrations measured in SAMHE schools, we next analyse them alongside the $\text{PM}_{2.5}$ concentrations of ambient outdoor air as measured at AURN sites (§3.1). The effect of periods of high outdoor $\text{PM}_{2.5}$ concentrations, or ‘outdoor $\text{PM}_{2.5}$ events’, on school $\text{PM}_{2.5}$ concentrations are examined in greater detail in §3.2. Finally, in §3.3, a gauge of the accumulated effect of varying $\text{PM}_{2.5}$ concentrations over the academic year is assessed by estimating the exposure received. The contribution that potential exposure during events had to the total exposure is also assessed.

3.1. Analysis of the SAMHE school and AURN outdoor $\text{PM}_{2.5}$ concentrations over the academic year

Across the academic year 2023–2024, the SAMHE $\text{PM}_{2.5}$ concentrations, measured by the SAMHE schools’ monitors, are well correlated with the AURN $\text{PM}_{2.5}$ concentration measurements from outdoors. By comparing the ‘schoolday datasets’ so that only periods when the schools were operational (and their buildings expected to be occupied and actively ventilated), i.e. the SAMHE and the AURN schoolday mean $\text{PM}_{2.5}$ concentrations are significantly correlated (illustrated in figure 2b), with a Spearman’s rank correlation coefficient of approximately 0.77, with a p-value of $p < 2.2 \times 10^{-16}$ — we note that the school and AURN measurements were not co-located and were separated by a mean distance of between 14 km and 20 km. Moreover, we note that the strong correlation is evident despite the many potential sources of $\text{PM}_{2.5}$ in school air, including numerous sources from schools’ activities.

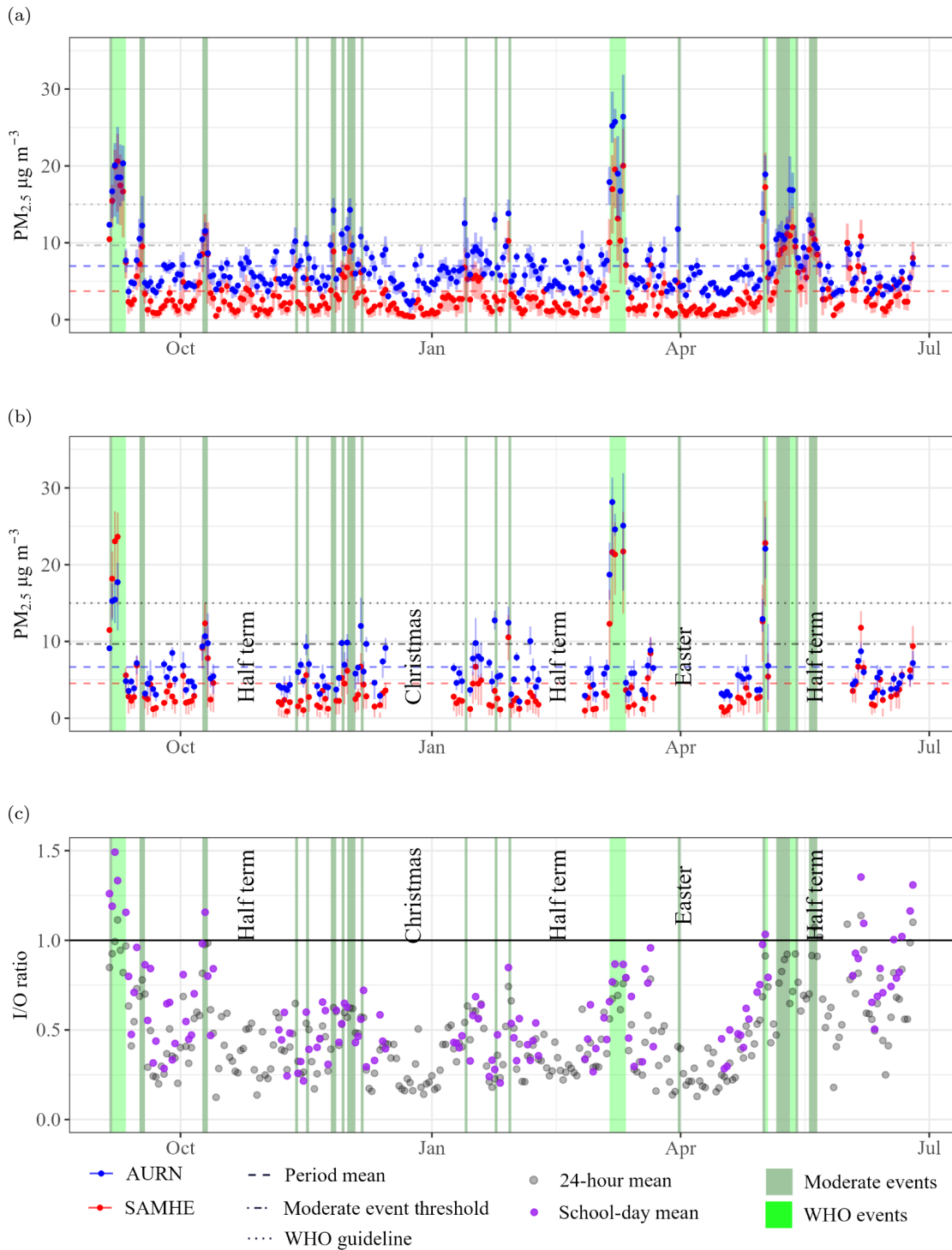


Figure 2: Time series illustrating the variation in $PM_{2.5}$ concentrations throughout the academic year 2023–2024 as measured by the SAMHE monitors in schools, and the AURN sites outdoors. Within (a), red circular markers indicate the average of, and the vertical bars indicate the interquartile range within, the 24-hour mean $PM_{2.5}$ concentration measurements across SAMHE schools' on each calendar day; blue circular markers and the vertical bars indicate the equivalent data from the AURN sites' measurements of ambient outdoor concentrations. Within (b), red circular markers indicate the average of, and the vertical bars indicate the interquartile range within, the schoolday mean $PM_{2.5}$ concentration measurements across SAMHE schools' on each schoolday; blue circular markers and the vertical bars indicate the equivalent from the AURN measurements outdoors. Within (c) the 'Indoor-outdoor ratio' of, appropriately averaged, school-outdoor concentrations: grey markers indicate the ratios based on the 24-hour mean $PM_{2.5}$ concentration measurements on each calendar day (i.e. the circular markers plotted in (a)), and purple markers indicate the ratios based on the schoolday mean $PM_{2.5}$ concentration measurements on each schoolday (i.e. the circular markers plotted in (b)). In each pane, the green vertical panels show periods when ' $PM_{2.5}$ events' occur, light green showing $PM_{2.5}$ events for which the outdoor concentration exceeded the WHO guideline and dark green for moderate $PM_{2.5}$ events.

Perhaps more surprisingly, during unoccupied days when, for security reasons, the schools’ windows and doors are expected to be closed, examination of figure 2a shows that the SAMHE 24-hour mean $\text{PM}_{2.5}$ concentrations do still reach elevated levels when the AURN 24-hour mean $\text{PM}_{2.5}$ concentrations are higher (the timing of these non-schooldays is evident on comparing the days for which data is plotted in figure 2a but no data is plotted in figure 2b). Examining the ‘continuous period datasets’ which include measurements made on non-schooldays and overnights the correlation between the SAMHE and AURN $\text{PM}_{2.5}$ concentration measurements remain strong and is not significantly different from that during the schooldays (the Spearman’s rank correlation is approximately 0.83, with a p-value of $p < 2.2 \times 10^{-16}$). This suggests that the building envelopes of the UK’s SAMHE schools are still relatively permeable to $\text{PM}_{2.5}$ even when windows and ventilation openings might be expected to be closed.

The SAMHE $\text{PM}_{2.5}$ concentrations examined, which are each means of the values recorded from within schools widely distributed across the UK (see figure 1), are well correlated with the AURN $\text{PM}_{2.5}$ concentrations (which are also each means of the values recorded at AURN sites across the UK, see also figure 1) — the datasets exhibiting such a clear correlation between the indoor school concentrations and the outdoor concentrations is noteworthy because of the scale of the datasets. As such, it is a notable finding that trends in $\text{PM}_{2.5}$ concentrations within UK schools are strongly linked to $\text{PM}_{2.5}$ concentrations in ambient outdoor air at a national scale.

There is a range of potential sources of particulate matter that can be generated in school classrooms, which include organic sources such as skin flakes and clothes fibres as well as chalk (where still used) and particles generated from building deterioration (Son, 2023; Amato et al., 2014; Becerra et al., 2020). Moreover, the concentration of $\text{PM}_{2.5}$ in classrooms has been found to be closely correlated to the activity level of pupils in the classroom, especially as occupant activity plays a key role in the re-suspension of settled particles, (Son, 2023; Becerra et al., 2020). It is desirable to estimate how much of the $\text{PM}_{2.5}$ measured in schools might be due to their production therein. To do this, we examine average $\text{PM}_{2.5}$ concentrations, within the two relevant periods, over the whole academic year. Taking the continuous period datasets, i.e. based on the 24-hour means and including non-schooldays, the average of the AURN data (measured outdoors) is $3.26 \mu\text{g}/\text{m}^3$ higher than that of the SAMHE data, measured in schools. However, when examining the schoolday datasets, i.e. based on the 09:00-16:00 means only on schooldays during which in-school sources are generated and there may also be a higher infiltration from outdoors, this difference falls to $2.14 \mu\text{g}/\text{m}^3$. This is a result that would be obtained if, all else remained equal and, during school hours the production of $\text{PM}_{2.5}$ indoors was sufficient to increase the $\text{PM}_{2.5}$ concentration by, on average, $1.12 \mu\text{g}/\text{m}^3$. This is significant finding, given that average of school-year SAMHE dataset over the whole academic year is $4.54 \mu\text{g}/\text{m}^3$ and we therefore assert that, a reasonable upper bound for, the fraction of $\text{PM}_{2.5}$ measured in schools that is due to sources within the schools, might be approximately 25%.

3.2. Examining the data through ‘ $\text{PM}_{2.5}$ event’ periods, based on outdoor concentrations

Our results (§3.1) evidence the strong correlation between outdoor and school $\text{PM}_{2.5}$ concentrations; consequently, we seek to investigate the impact of periods of high outdoor $\text{PM}_{2.5}$ concentrations, herein ‘ $\text{PM}_{2.5}$ events’, on the concentrations measured in schools. As described (§2.2.2), $\text{PM}_{2.5}$ events are defined as any day, or set of consecutive days, when the AURN 24-hour mean $\text{PM}_{2.5}$ concentration exceeds some threshold value, herein we investigate two event types based on two differing threshold values, namely: “WHO $\text{PM}_{2.5}$ events” defined based on a threshold value of $15 \mu\text{g}/\text{m}^3$ (taking the 24-hour mean health-based limit recommended by the World Health Organisation, WHO), and “Moderate $\text{PM}_{2.5}$ events” for which the threshold is set to be the median plus, one standard deviation, of the ‘continuous period AURN dataset’, this threshold has the value of $9.67 \mu\text{g}/\text{m}^3$. The median being selected since it is less affected by outliers than the mean, but we note that threshold is entirely dependent on the measured concentrations, unlike that for WHO $\text{PM}_{2.5}$ events. Moreover, any particular threshold could have been chosen, the choice being somewhat arbitrary; however, in choosing a smaller value than the WHO guideline, Moderate $\text{PM}_{2.5}$ events seek to analyse the impact on school air quality of the more frequent but less extreme outdoor $\text{PM}_{2.5}$ events.

Identifying particular $\text{PM}_{2.5}$ events enables examination of the climatic conditions associated with their occurrence. Analysis of air-mass back trajectories (see Appendix E for a full description of the method

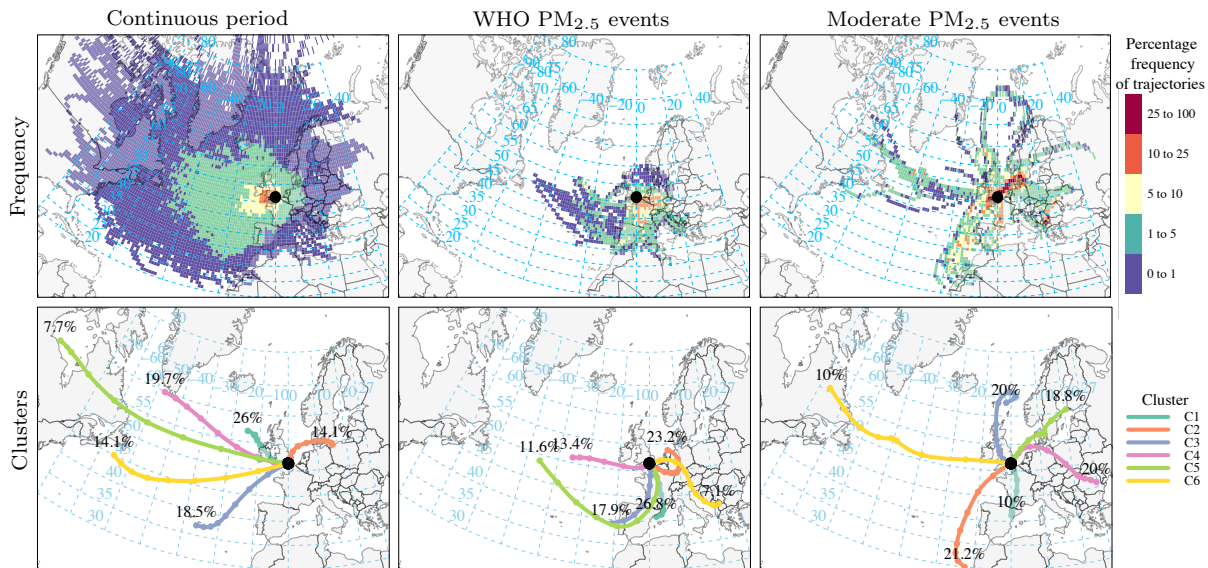


Figure 3: Illustration of the (four-day) air-mass back trajectories arriving at the London Honor Oak Park AURN site (each calculated at three-hour intervals), segregated based on arrival times during: a) the whole duration of the continuous period (first column), b) during WHO $PM_{2.5}$ events (second column), and c) during moderate $PM_{2.5}$ events (third column). The first row indicates, though the colour shading, the frequency with which the trajectories passed through the longitude-latitude grid cells. The second row shows the results of the cluster analysis (see Appendix E for details) for the respective trajectories.

employed) was also carried out to, where possible, infer where sources of $PM_{2.5}$ might have geographically originated from. A ‘trajectory’ is based on simplified weather data and represents the movement of the centroid of a mass of air over a number of days. Back trajectories indicate where air-masses that arrived at a specific location and time, might have originated from (for a comprehensive description of trajectories and their calculation see Fleming et al., 2012). The trajectories are calculated throughout the continuous period and just for the periods of time during which events occurred. Comparisons of the trajectories during events to the trajectories during the whole continuous period are made to identify if there are particular origins of air masses associated with outdoor $PM_{2.5}$ events and elevated $PM_{2.5}$ concentrations in schools. Trajectories also reveal the speed at which air masses move, slow moving air masses may allow for more local pollutants to accumulate. For our purposes, it was important to determine if the back trajectories of air-masses arriving at a single location in the UK might be broadly representative of those air-masses arriving elsewhere in the UK. As such, we calculated trajectories at a location in the south of the country, at London Honor Oak Park AURN site, and at a location in the north of the country, Auchencorth Moss AURN site, located south of Edinburgh. The analysis of trajectories at these two locations were qualitatively compared and found to reveal similar air-mass trajectories. For convenience of presentation, only the trajectories for the London Honor Oak site are presented herein.

3.2.1. WHO $PM_{2.5}$ events

During the continuous period (academic year 2023–2024) four WHO $PM_{2.5}$ events occurred. These are highlighted by the vertical light-green panels in figure 2, and the dates are summarised in table F.1. Elevated levels of $PM_{2.5}$ concentration are evident in schools during all of the WHO $PM_{2.5}$ events (e.g. see figures 2a and 2b, with the associated indoor measurement themselves typically exceeding the WHO threshold. The indoor-outdoor ratio during the first WHO $PM_{2.5}$ event, during September, is significantly higher than during the other events. This period of time coincided with the start of the school term for English and Welsh schools, and it is possible that a greater amount of dust, that had settled over the summer holiday, might have been re-suspended by activities on these schooldays — a hypothesis loosely supported by the

indoor-outdoor ratio, during this WHO PM_{2.5} event, being greater based on the schoolday means than that of the 24-hour means. On the day following each WHO PM_{2.5} event, the SAMHE schoolday mean PM_{2.5} concentration reduced below the threshold, indicating the residence time of the PM_{2.5} within schools is not longer than a day.

The second column of figure 3 shows that the back trajectories of air-masses arriving in London during the WHO PM_{2.5} events have (over the four days prior to their arrival) predominantly spent time over Europe; mostly over France, Belgium and Germany. By contrast, the first column of figure 3 shows that, averaged over the whole continuous period, the trajectories more frequently arrive from over the Atlantic Ocean where there are relatively few sources of PM_{2.5} and are very different to those determined for WHO PM_{2.5} events. The air-masses that arrived during WHO PM_{2.5} events could have carried sources of PM_{2.5} generated in Northern Europe to the UK, as has been recorded to frequently occur in the past (Harrison et al., 2012; Malley et al., 2016; Graham et al., 2020). During PM_{2.5} events, it is likely that a pupil will be exposed to an elevated concentration of PM_{2.5} whether they are at school, home or in another environment. The events of the academic year 2023—2024 had a seasonal occurrence corresponding with the trends reported in previous years in the aforementioned studies. These PM_{2.5} events occur more frequently during winter and spring, for which the proportion of time spent by pupils in school is greater than during the summer, which is comprised of the long summer holidays. Therefore, the operation and management of school environments are important when considering mitigating actions to reduce exposure received during PM_{2.5} events. Indeed, similar seasonal instances of PM_{2.5} events may occur in future academic years, which could also lead to elevated concentrations of PM_{2.5} in schools.

3.2.2. Moderate PM_{2.5} events

Based on our definition and data, a ‘moderate’ outdoor PM_{2.5} event occurred when the outdoor 24-hour mean PM_{2.5} concentration exceeded $9.67 \mu\text{g}/\text{m}^3$ — the median plus one standard deviation of the continuous period AURN dataset (indicated by the dot-dash lines in figure 2). There were 17 periods when a moderate PM_{2.5} event was determined to have occurred, as shown by the dark green panels in figure 2. Note that some of these PM_{2.5} events occur on the days before and after some of the WHO PM_{2.5} events. The dates of the 17 moderate PM_{2.5} events recorded are summarised in table F.2 which also shows that whilst these PM_{2.5} events occurred over 28 days, only ten of these were schooldays. Most of the moderate PM_{2.5} events are of shorter duration relative to the WHO PM_{2.5} events.

Elevated PM_{2.5} concentrations are detected in schools during these moderate PM_{2.5} event. However, only during four moderate PM_{2.5} events (out of 17) did a SAMHE schoolday mean PM_{2.5} concentration exceed the threshold, *cf.* the WHO PM_{2.5} events. Consistent with the WHO PM_{2.5} event data, even if an event raised the PM_{2.5} concentration in schools over a weekend, the effect of the event is typically not evident on the following schoolday.

The clustered back trajectories of air-masses arriving into London during the moderate PM_{2.5} events, as shown in the third column of figure 3, are distinctly different to those during WHO PM_{2.5} events (shown in the second column), indicating that the conditions that cause elevated AURN PM_{2.5} concentrations are not common to both types of events. Air-masses that travel over Europe during moderate PM_{2.5} events are described by 48.8% of the clustered trajectories, as compared with 86.6% of trajectories during WHO PM_{2.5} events. Unlike during WHO PM_{2.5} events, air-masses travel over parts of the UK and more frequently over the Atlantic ocean. Clustered trajectories that travel over the Atlantic, which typically introduce little to no PM_{2.5} to the air-masses, represent 31.2% of trajectories during moderate PM_{2.5} events. The clustered trajectories that travel over the UK during moderate PM_{2.5} events are shorter than other trajectories, showing the air-masses associated with these trajectories were slower moving, which would allow sources to accumulate in the outdoor air of the UK. A higher proportion of trajectories travelling over the Atlantic and slow moving air-masses over the UK would suggest that sources of PM_{2.5} generated within the UK contribute significantly to causing moderate PM_{2.5} events.

3.3. Exploring the implication by examining the exposure potential

School air quality is important because of the potential for relatively long duration exposures to occur there. As such, we calculate estimates of the potential exposure of PM_{2.5} that might, on average, be received

in a school. For each minute of every schoolday, an average concentration, C ($\mu\text{g m}^{-3}$), is calculated from the $\text{PM}_{2.5}$ concentrations measured at included schools. From this, an estimate of potential exposure (μg) is calculated on each schoolday by integrating the product of C and an average breathing rate, Q_b , over the duration of the school day. For the breathing rate, we take $Q_b = 0.012 \text{ m}^3 \text{ min}^{-1}$, based on the average breathing rate of children with ages in the range [6,16] doing light intensity activity, as recommended for short-term inhalation exposures, see EPA (2011). Herein, SAMHE $\text{PM}_{2.5}$ concentrations of minutely frequency are used, Appendix C discusses the consequences of using hourly or daily averaged data.

The total potential exposure over the entire school-year was estimated to be 3 041 μg . The contribution to the total exposure from different concentration ranges, segregated into discrete concentration bins of 1 $\mu\text{g}/\text{m}^3$ in width, is shown in figure 4a. Two distinct modes exist, below and above 15 $\mu\text{g}/\text{m}^3$ (coincidentally the WHO guideline threshold value), and most of the potential exposure over a school-year is due to $\text{PM}_{2.5}$ exposures during non-event days, i.e. on days for which the mean of the AURN dataset remained below the threshold of its median plus one standard deviation — these constitute the majority of days.

The potential exposure during $\text{PM}_{2.5}$ events is simply calculated by summing the potential exposures associated with each schoolday on which the relevant $\text{PM}_{2.5}$ event criteria was satisfied. The contribution of different concentrations to the potential exposure associated with $\text{PM}_{2.5}$ events is overlaid in figure 4a as green bars. Since moderate $\text{PM}_{2.5}$ events are defined when that day’s AURN 24-hour mean $\text{PM}_{2.5}$ concentration exceeds 9.67 $\mu\text{g}/\text{m}^3$ and §3.1 evidences strong correlations between concentrations outdoors and those in school, it is not surprising that during events the potential exposure is associated elevated with elevated concentrations within the schools, with most of the contribution to exposure associated with concentrations greater than 15 $\mu\text{g}/\text{m}^3$. It is also notable from figure 4a that some of the potential exposure associated with high concentrations in schools does occur outside of $\text{PM}_{2.5}$ events.

Although the majority of the total potential exposure over a school-year is estimated outside of $\text{PM}_{2.5}$ events, the exposure received during $\text{PM}_{2.5}$ events is significant — our estimates indicate they contribute 41% of the total potential exposure whilst only occurring on 13% of days. The exposure received during WHO $\text{PM}_{2.5}$ events is more significant still, exacerbated by their relatively long durations. WHO $\text{PM}_{2.5}$ events contribute 27% of the total potential exposure and account for 6% of the school-year; moderate $\text{PM}_{2.5}$ events account for 14% of the total potential and occurred on 7% of the school-year. We note that the potential exposure calculations only consider the exposure received whilst pupils are at school. This can be a significant proportion of their exposure (some estimates suggest that 30%–40% of a yearly-averaged child’s daily (24-hour period) exposure is received in the classroom Rivas et al., 2016; Faria et al., 2020); however, children are exposed to $\text{PM}_{2.5}$ in other indoor environments as well as outdoors, most notably whilst commuting to and from school (Correia et al., 2020; Varaden et al., 2019; Nieuwenhuijsen et al., 2015). Additionally, outdoor $\text{PM}_{2.5}$ events more frequently occur during the school-year than during the summer holidays (Kelly et al., 2023; Abdalmogith and Harrison, 2005), the longest period for which pupils are not in school. As such, the contribution of outdoor $\text{PM}_{2.5}$ events to a child’s total potential exposure over the entire calendar year (September 2023 to August 2024) would be considerably lower.

4. Conclusions

Analysis of the concentrations of $\text{PM}_{2.5}$ recorded by 490 SAMHE monitors in schools, across the UK, during the academic year 2023–2024 were reported. Local and regional variations in ambient outdoor $\text{PM}_{2.5}$ concentrations are well documented (Harrison et al., 2012), despite these, and the likely variation in activities and air quality between classrooms (Burridge et al., 2023), significant correlations in classroom $\text{PM}_{2.5}$ were evident on a national scale— indicating that large-scale pollution events across the nation have a significant impact on classroom air quality. During periods of elevated ambient outdoor $\text{PM}_{2.5}$ concentrations — outdoor $\text{PM}_{2.5}$ events — the concentration in schools was also found to be significantly elevated. The data showed that these included events where the 24-hour mean health-based limit (15 $\mu\text{g}/\text{m}^3$) recommended by the World Health Organisation was exceeded within schools. These WHO $\text{PM}_{2.5}$ events have a significant impact on the long-term exposure over a school-year, contributing to 27% of the total potential exposure whilst only occurring on 6% of the schooldays over the year. Back trajectory analysis reveals that the WHO $\text{PM}_{2.5}$ events analysed are caused by transboundary sources which have specific geographical locations and

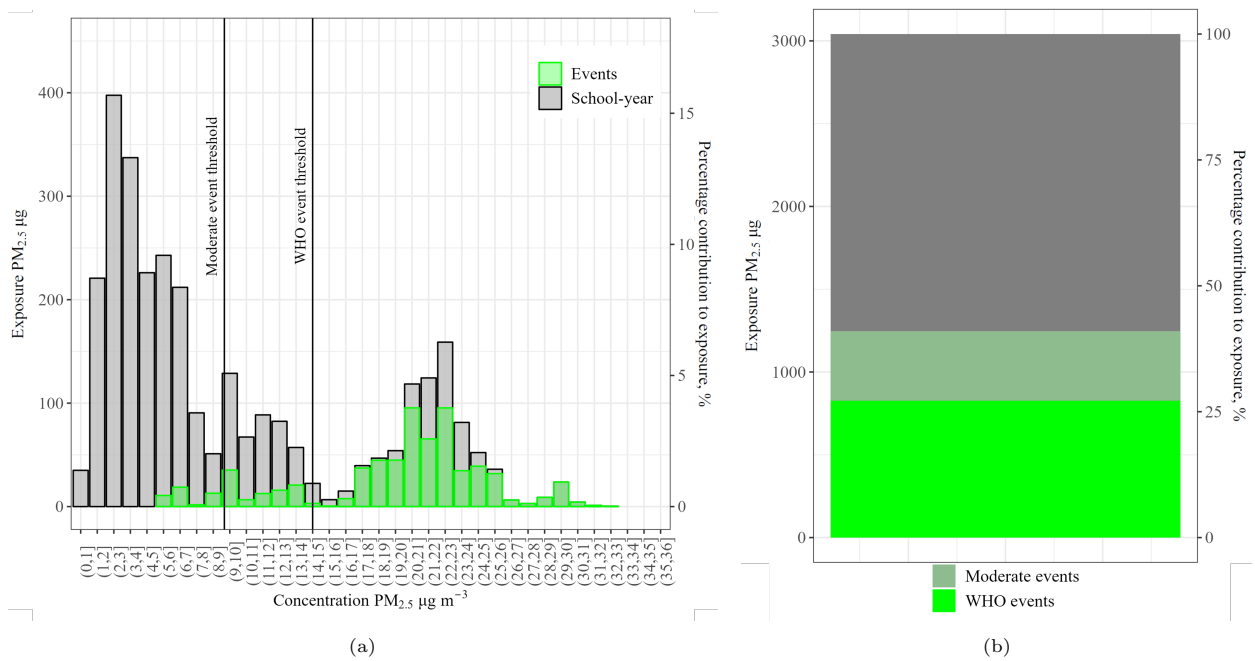


Figure 4: (a) Grey bars indicate the contribution to the total potential exposure during the school-year apportioned, into $1 \mu g/m^3$ wide bins, by the minutely SAMHE $PM_{2.5}$ concentrations, overlaid in green are those associated with $PM_{2.5}$ event periods. Vertical black lines mark the values of the $PM_{2.5}$ events thresholds. (b) Bar chart showing the total potential dosage over the school-year: the bright-green region indicates the potential dosage associated with WHO $PM_{2.5}$ events, the dark-green region that associated with moderate events, and the grey region indicates potential dosage associated with day outside of $PM_{2.5}$ events.

are typically brought to the UK by westerly winds. However, sources generated in the UK can also lead to elevated concentrations of PM_{2.5} outdoors and in schools, especially when air masses over the UK are slow-moving, allowing sources of PM_{2.5} to accumulate. In mitigating children’s exposure to PM_{2.5}, some consideration could be devoted to periods of elevated outdoor PM_{2.5} concentrations; for example, when PM_{2.5} pollution forecasts are high, changes in the operation of school ventilation or air cleaners/filters (noting that any reduction in ventilation risk increasing pollution from indoor sources, including respiratory aerosols) could be considered as a response. However, we note that any suggestion of a response to such periods involving a reduction in attendance at schools, risks increasing children’s exposures elsewhere (e.g. in homes where cooking and sources of combustion are more prevalent and infiltration of outdoor sources also occurs) and would negatively impact on their education and socialisation.

We conclude that, whilst there are significant indoor sources of PM_{2.5} in schools, PM_{2.5} incoming as outdoor air ventilates schools and classrooms appears to be the major source. School buildings in the UK are permeable to PM_{2.5}, even when unoccupied and ventilation openings are expected closed, and this has serious implications for schools’ heating costs in the context of the UK government’s Net Zero Strategy. This study further highlights the need for continued longitudinal measurements of air quality in schools, and other indoor spaces, which may provide insights into the impact of seasonal pollution patterns on air quality indoors, with potential to evidence the need, and identify efficient routes, to mitigate.

Acknowledgements

The authors would like to thank all of the schools, teachers and pupils who have participated in the SAMHE project, and acknowledge the contribution of everyone involved, including members of the SAMHE Steering Committee and SAMHE Engagement Panel, for their continued support and guidance.

The authors are grateful to Anika Krause, Sirel Saladin and Achim Haug from AirGradient who have provided support with the evaluation of associated errors with using low-cost sensors and sharing co-location data without which the co-location analysis would not be possible. The insightful comments of Professors Jacqui Hamilton, Pia Hardelid, Cath Noakes, Mark Mon Williams and Pawel Wargocki, and Drs Douglas Booker and Corinne Mandin are gratefully acknowledged, especially with regards critic of the error analysis.

The SAMHE Project Consortium members consist of the following, Imperial College London: Ben Barratt, Henry Burridge, Alice Handy, Christopher Pain, Kat Roberts, Samuel Wood; Stockholm Environment Institute, University of York: Rhys Archer, Victoria Beale, Sam Bland, Douglas Wang, Lucy Way, Sarah West; UK Health Security Agency (UKHSA): Holly Carter, Dale Weston, Natalie Williams; University of Cambridge: Hannah Edwards, Paul Linden, Mark Winterbottom; University of Sheffield: Carolanne Vouriot; University of Leeds: Chris Brown, Marco-Felipe King, Mark Mon-Williams; University of Surrey: Sarkawt Hama, Prashant Kumar.

Funding

The ‘School Air quality Monitoring for Health and Education’ project, SAMHE — an extension of the CO-TRACE project, was funded by the EPSRC under grant number EP/W001411/1, and received additional funding from the UK’s Department for Education.

Data Statement

The authors do not have permission to share data.

References

- K.-H. Kim, E. Kabir, S. Kabir, A review on the human health impact of airborne particulate matter, *Environment international* 74 (2015) 136–143. doi:[10.1016/j.envint.2014.10.005](https://doi.org/10.1016/j.envint.2014.10.005).
- K. Exley, S. Dimitroulopoulou, A. Gowers, T. Waite, A. Hansell, Chief Medical Officer’s Annual Report 2022 Air Pollution: Chapter 1 – Air pollution and health; Air pollution and how it harms health (2022).

- N. Rees, Danger in the air: How air pollution can affect brain development in young children, Technical Report, United Nations Children's Fund, 2017.
- Y.-S. Son, A review on indoor and outdoor factors affecting the level of particulate matter in classrooms of elementary schools, *Journal of Building Engineering* 75 (2023) 106957. doi:10.1016/j.jobe.2023.106957.
- T. Zhang, Y. Wu, Y. Guo, B. Yan, J. Wei, H. Zhang, X. Meng, C. Zhang, H. Sun, L. Huang, Risk of illness-related school absenteeism for elementary students with exposure to PM_{2.5} and O₃, *Science of The Total Environment* 842 (2022) 156824. doi:10.1016/j.scitotenv.2022.156824.
- P. Wargocki, J. A. Porras-Salazar, S. Contreras-Espinoza, W. Bahnfleth, The relationships between classroom air quality and children's performance in school, *Building and Environment* 173 (2020) 106749. doi:10.1016/j.buildenv.2020.106749.
- S. Sadrizadeh, R. Yao, F. Yuan, H. Awbi, W. Bahnfleth, Y. Bi, G. Cao, C. Croitoru, R. de Dear, F. Haghighat, P. Kumar, M. Malayeri, F. Nasiri, M. Ruud, P. Sadeghian, P. Wargocki, J. Xiong, W. Yu, B. Li, Indoor air quality and health in schools: A critical review for developing the roadmap for the future school environment, *Journal of Building Engineering* 57 (2022) 104908. doi:10.1016/j.jobe.2022.104908.
- T. Faria, V. Martins, C. Correia, N. Canha, E. Diapouli, M. Manousakas, K. Eleftheriadis, S. M. Almeida, Children's exposure and dose assessment to particulate matter in Lisbon, *Building and Environment* 171 (2020) 106666. doi:10.1016/j.buildenv.2020.106666.
- WHO, WHO global air quality guidelines: particulate matter (PM_{2.5} and PM₁₀), ozone, nitrogen dioxide, sulfur dioxide and carbon monoxide, World Health Organization, 2021.
- F. Amato, I. Rivas, M. Viana, T. Moreno, L. Bouso, C. Reche, M. Álvarez-Pedrerol, A. Alastuey, J. Sunyer, X. Querol, Sources of indoor and outdoor PM_{2.5} concentrations in primary schools, *Science of The Total Environment* 490 (2014) 757–765. doi:10.1016/j.scitotenv.2014.05.051.
- J. A. Becerra, J. Lizana, M. Gil, A. Barrios-Padura, P. Blondeau, R. Chacartegui, Identification of potential indoor air pollutants in schools, *Journal of Cleaner Production* 242 (2020) 118420. doi:10.1016/j.jclepro.2019.118420.
- O. Poupard, P. Blondeau, V. Iordache, F. Allard, Statistical analysis of parameters influencing the relationship between outdoor and indoor air quality in schools, *Atmospheric Environment* 39 (2005) 2071–2080. doi:10.1016/j.atmosenv.2004.12.016.
- S. Stamp, E. Burman, L. Chatzidiakou, E. Cooper, Y. Wang, D. Mumovic, A critical evaluation of the dynamic nature of indoor-outdoor air quality ratios, *Atmospheric Environment* 273 (2022) 118955. doi:10.1016/j.atmosenv.2022.118955.
- M. Mohammadyan, A. Alizadeh-Larimi, S. Etemadinejad, M. T. Latif, B. Heibati, K. Yetilmeszooy, S. A. Abdul-Wahab, P. Dadvand, Particulate Air Pollution at Schools: Indoor-Outdoor Relationship and Determinants of Indoor Concentrations, *Aerosol and Air Quality Research* 17 (2017) 857–864. doi:10.4209/aaqr.2016.03.0128.
- R. M. Harrison, D. Laxen, S. Moorcroft, K. Laxen, Processes affecting concentrations of fine particulate matter (PM_{2.5}) in the UK atmosphere, *Atmospheric Environment* 46 (2012) 115–124. doi:10.1016/j.atmosenv.2011.10.028.
- L. Chatzidiakou, R. Archer, V. Beale, S. Bland, H. Carter, C. Castro-Faccetti, H. Edwards, J. Finneran, S. Hama, R. L. Jones, P. Kumar, P. F. Linden, N. Rawat, K. Roberts, C. Symons, C. Vouriot, D. Wang, L. Way, S. West, D. Weston, N. Williams, S. Wood, H. C. Burrige, Schools' air quality monitoring for health and education: Methods and protocols of the SAMHE initiative and project, *Developments in the Built Environment* 16 (2023) 100266. doi:10.1016/j.dibe.2023.100266.
- S. E. West, L. Way, R. Archer, V. J. Beale, S. Bland, H. Burrige, C. Castro-Faccetti, L. Chatzidiakou, P. Kumar, C. Vouriot, N. Williams, SAMHE Project Consortium, Co-Designing an Air Quality Web App with School Pupils and Staff: The SAMHE Web App, *Citizen Science: Theory and Practice* 8 (2023) 64. doi:10.5334/cstp.620.
- HM Government, UK, BB 101: Guidelines on ventilation, thermal comfort, and indoor air quality in schools (2018).
- R. Duvall, A. Clements, G. Hagler, A. Kamal, V. Kilaru, L. Goodman, S. Frederick, K. Barkjohn, I. VonWald, D. Greene, et al., Performance testing protocols, metrics, and target values for fine particulate matter air sensors: use in ambient, outdoor, fixed site, non-regulatory supplemental and informational monitoring applications, US EPA Office of Research and Development (2021).
- Defra AURN, 2024, AURN site classification, URL: <https://uk-air.defra.gov.uk/networks/site-types>.
- AirGradient, Does the EPA Correction Algorithm for Wildfire Smoke PM_{2.5} Developed for PurpleAir Work for AirGradient Monitors?, 2024. URL: <https://www.airgradient.com/blog/epa-correction-and-airgradient/>.
- S. Hama, P. Kumar, A. Tiwari, Y. Wang, P. F. Linden, The Underpinning Factors Affecting the Classroom Air Quality, Thermal Comfort and Ventilation in 30 Classrooms of Primary Schools in London, *Environmental Research* 236 (2023) 116863. doi:10.1016/j.envres.2023.116863.
- European Commission, Joint Research Centre, Directorate-General for Health and Consumers, Institute for Health and Consumer Protection, M. Varró, A. Hyvärinen, P. Rudnai, T. Pándics, J. Madureira, A. Páldy, H. Moshammer, J. Barrero-Moreno, E. Csobod, M. Täubel, M. Stranger, D. Norback, I. Annesi-Maesano, G. Ventura, E. Oliveira Fernandes, E. Vaskovi, T. Beregszászi, P. Sestini, G. Viegi, P. Carrer, S. Kephelopoulou, SINPHONIE – Schools Indoor Pollution & Health Observatory Network in Europe – Final Report, Publications Office, 2014. URL: <https://data.europa.eu/doi/10.2788/99220>.
- DEFRA, Particulate matter (PM₁₀/PM_{2.5}), Air quality statistics in the UK, 1987 to 2023 - Particulate matter (PM₁₀/PM_{2.5}), 2024. URL: <https://www.gov.uk/government/statistics/air-quality-statistics/concentrations-of-particulate-matter-pm10-and-pm25>, Department for Environment Food and Rural Affairs.
- EEA, Air quality in Europe — 2013 report, Technical Report, European Environment Agency, 2013. URL: <https://www.eea.europa.eu/publications/air-quality-in-europe-2013>, European Environment Agency, ISSN 1725-9177.
- EEA, Europe's air quality status 2024, 2024. URL: <https://www.eea.europa.eu/publications/europes-air-quality-status-2024>, European Environment Agency.
- Z. L. Fleming, P. S. Monks, A. J. Manning, Untangling the influence of air-mass history in interpreting observed atmospheric composition, *Atmospheric Research* 104 (2012) 1–39. doi:10.1016/j.atmosres.2011.09.009.
- C. S. Malley, M. R. Heal, C. F. Braban, J. Kentisbeer, S. R. Leeson, H. Malcolm, J. J. N. Lingard, S. Ritchie, R. Maggs,

	First day of term	Last day of term	No of days	No of schooldays
Autumn term before half-term	5th September	13th October	39	29
Autumn term after half-term	6th November	15th December	40	30
Spring term before half-term	9th January	9th February	32	24
Spring term after half-term	26th February	22nd March	26	20
Summer term before half-term	16th April	3rd May	18	14
Summer term after half-term	3rd June	25th June	23	17

Table A.1: School terms that make up what is considered the school-year within this study.

- S. Beccaceci, P. Quincey, R. J. C. Brown, M. M. Twigg, The contributions to long-term health-relevant particulate matter at the UK EMEP supersites between 2010 and 2013: Quantifying the mitigation challenge, *Environment International* 95 (2016) 98–111. doi:[10.1016/j.envint.2016.08.005](https://doi.org/10.1016/j.envint.2016.08.005).
- A. M. Graham, K. J. Pringle, S. R. Arnold, R. J. Pope, M. Vieno, E. W. Butt, L. Conibear, E. L. Stirling, J. B. McQuaid, Impact of weather types on UK ambient particulate matter concentrations, *Atmospheric Environment: X* 5 (2020) 100061. doi:[10.1016/j.aeaao.2019.100061](https://doi.org/10.1016/j.aeaao.2019.100061).
- EPA, Exposure Factors Handbook: 2011 Edition, Technical Report EPA/600/R-09/052F, U.S. Environmental Protection Agency (EPA), 2011.
- I. Rivas, D. Donaire-Gonzalez, L. Bouso, M. Esnaola, M. Pandolfi, M. de Castro, M. Viana, M. Álvarez-Pedrerol, M. Nieuwenhuijsen, A. Alastuey, J. Sunyer, X. Querol, Spatiotemporally resolved black carbon concentration, schoolchildren’s exposure and dose in Barcelona, *Indoor Air* 26 (2016) 391–402. doi:[10.1111/ina.12214](https://doi.org/10.1111/ina.12214).
- C. Correia, V. Martins, I. Cunha-Lopes, T. Faria, E. Diapouli, K. Eleftheriadis, S. M. Almeida, Particle exposure and inhaled dose while commuting in Lisbon, *Environmental Pollution* 257 (2020) 113547. doi:[10.1016/j.envpol.2019.113547](https://doi.org/10.1016/j.envpol.2019.113547).
- D. Varaden, E. Leidland, B. Barratt, The Breathe London wearables study: engaging primary school children to monitor air pollution in London, Technical Report, King’s College London Environmental Research Group, 2019.
- M. J. Nieuwenhuijsen, D. Donaire-Gonzalez, I. Rivas, M. de Castro, M. Cirach, G. Hoek, E. Seto, M. Jerrett, J. Sunyer, Variability in and Agreement between Modeled and Personal Continuously Measured Black Carbon Levels Using Novel Smartphone and Sensor Technologies, *Environmental Science & Technology* 49 (2015) 2977–2982. doi:[10.1021/es505362x](https://doi.org/10.1021/es505362x).
- J. M. Kelly, E. A. Marais, G. Lu, J. Obszynska, M. Mace, J. White, R. J. Leigh, Diagnosing domestic and transboundary sources of fine particulate matter (PM_{2.5}) in UK cities using GEOS-Chem, *City and Environment Interactions* 18 (2023) 100100. doi:[10.1016/j.cacint.2023.100100](https://doi.org/10.1016/j.cacint.2023.100100).
- S. S. Abdalmogith, R. M. Harrison, The use of trajectory cluster analysis to examine the long-range transport of secondary inorganic aerosol in the UK, *Atmospheric Environment* 39 (2005) 6686–6695. doi:[10.1016/j.atmosenv.2005.07.059](https://doi.org/10.1016/j.atmosenv.2005.07.059).
- H. C. BurrIDGE, S. Bontitsopoulos, C. Brown, H. Carter, K. Roberts, C. Vouriot, D. Weston, M. Mon-Williams, N. Williams, C. Noakes, Variations in classroom ventilation during the COVID-19 pandemic: Insights from monitoring 36 naturally ventilated classrooms in the UK during 2021, *Journal of Building Engineering* 63 (2023) 105459. doi:[10.1016/j.job.2022.105459](https://doi.org/10.1016/j.job.2022.105459).
- A. F. Stein, R. R. Draxler, G. D. Rolph, B. J. B. Stunder, M. D. Cohen, F. Ngan, NOAA’s HYSPLIT Atmospheric Transport and Dispersion Modeling System, *Bulletin of the American Meteorology Society (BAMS)* (2015). doi:[10.1175/BAMS-D-14-00110.1](https://doi.org/10.1175/BAMS-D-14-00110.1).
- R. Kistler, E. Kalnay, W. Collins, S. Saha, G. White, J. Woollen, M. Chelliah, W. Ebisuzaki, M. Kanamitsu, V. Kousky, H. van den Dool, R. Jenne, M. Fiorino, The NCEP–NCAR 50-Year Reanalysis: Monthly Means CD-ROM and Documentation, *Bulletin of the American Meteorology Society (BAMS)* (2001).
- D. C. Carslaw, K. Ropkins, Openair — An R package for air quality data analysis, *Environmental Modelling & Software* 27–28 (2012) 52–61. doi:[10.1016/j.envsoft.2011.09.008](https://doi.org/10.1016/j.envsoft.2011.09.008).
- Q. Inc, Product specification sheet modulartm, 2023. URL: <https://assets.quant-aq.com/downloads/spec-sheets/modulair.latest.pdf>.
- D. Giavarina, Understanding bland altman analysis, *Biochemia medica* 25 (2015) 141–151.

Appendix A. School term dates

The dates of school terms and holidays differ between Scotland, Northern Ireland, and England and Wales. A set of dates was chosen to define the schoolday datasets by first defining ‘schools terms’ within which schools in all four nations might be active, with pupils in attendance, during the school week (Monday to Friday). The dates used to define these ‘terms’ are summarised in table A.1. Thereafter, any public holiday, within any of the four nations, falling within there ‘terms’ was further excluded from the schoolday datasets.

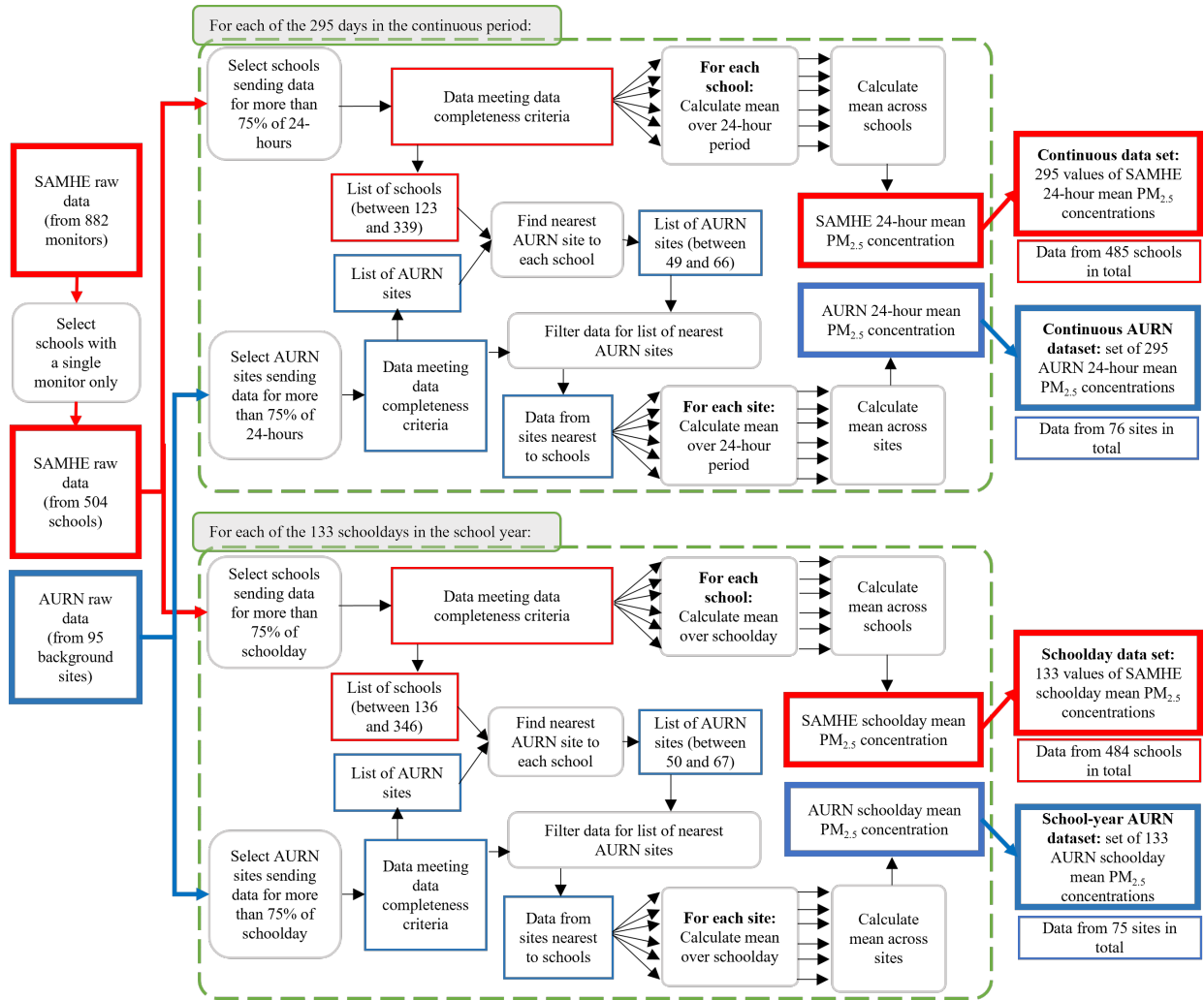


Figure B.1: A flow diagram summarizing the process through which the continuous period dataset and school-year datasets are formed. The red boxes represent data from SAMHE monitors, blue boxes represent data from AURN sites, and grey boxes show the processes applied to this data. The processes within the green dashed boxes are repeated for each day and schoolday in the continuous and school-year periods, respectively.

Appendix B. Formation of the analysable datasets

The process by which data is selected from SAMHE monitors to form the SAMHE continuous and schoolyear dataset is described in §2.2.1, and represented in the flow chart of figure B.1 by the red boxes. The formation of the AURN continuous and school-year datasets is described in §2.2.2 and represented by the blue boxes in figure B.1. Some schools within the SAMHE initiative, which are part of a HEPA filter intervention study, happen to have more than one monitor per school, but are not included in the analysis of this paper due to the presence of the HEPA filter intervention. From the 882 monitors that reported data over the academic year, 504 were in schools eligible for consideration, i.e. outside of the HEPA filter intervention study.

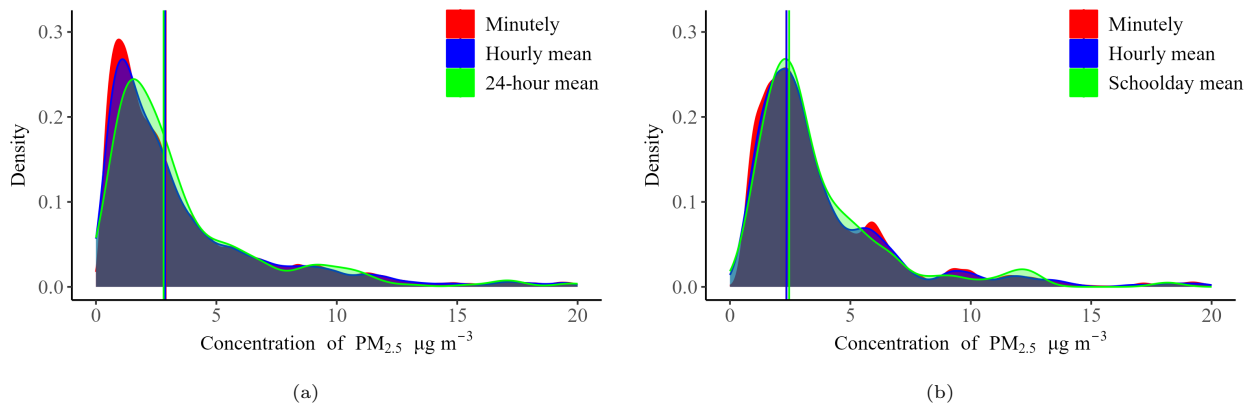


Figure C.2: (a) The probability density functions for the continuous period SAMHE dataset with differing averaging periods: minutely (red), hourly (blue), and 24-hour mean (green); (b) the equivalent for the SAMHE schoolday data. In each, vertical lines mark the median values of each distribution, which are effectively coincident for the minutely, and hourly-averaged, data.

Appendix C. Evaluation of the impact of varied time resolution

With access to minutely $\text{PM}_{2.5}$ concentration measurements on which to construct the SAMHE datasets, we explore the impact of time averaging the data over differing periods. For example, herein the primary datasets were constructed by taking the data from each included SAMHE monitor and averaging over a 24-hour period in the case of the continuous dataset, and the school day (09:00-16:00) in the case of the schoolday dataset — and then, in both cases, averaging across the included SAMHE schools. However, one could equally construct datasets by taking the data from each included SAMHE monitor (that satisfy the primary data completeness criteria) and averaging over a period of one-hour, or take the minutely data, and, again, in all cases then average over the SAMHE included schools — the latter creating datasets of “SAMHE minutely $\text{PM}_{2.5}$ concentration” (which prove of value when assessing the potential exposure, see below). Figure C.2 shows probability density functions associated with three different averaging periods (the primary data in green, hourly minutely in blue, and minutely in red) for: (a) the continuous period data, and (b) the schoolday data. Whilst figure C.2a does indicate some differences, e.g. the peak (modal) values of the SAMHE 24-hour mean $\text{PM}_{2.5}$ concentration distributions, table C.1 shows the key metrics of the distributions differ insignificantly in all cases. We therefore conclude that analysis of SAMHE 24-hour mean $\text{PM}_{2.5}$ concentrations (i.e. the SAMHE continuous datasets) and SAMHE schoolday mean $\text{PM}_{2.5}$ concentrations (i.e. the SAMHE schoolday datasets) is appropriate and is presented herein.

The potential exposure that pupils might receive was estimated using SAMHE minutely $\text{PM}_{2.5}$ concentrations, rather than SAMHE $\text{PM}_{2.5}$ concentrations over some longer period. To investigate the sensitivity of the finding to that choice, we compare the probability density of potential exposure as a function of concentration. Figure C.3 shows the contribution to the total potential exposure from different concentrations, segregated into discrete concentration bins of $1 \mu\text{g}/\text{m}^3$ width. The distribution of potential exposure is shown for the primary (minutely) SAMHE data (red), with the distributions overlain for the results based on hourly averaging (blue), and averaging over the schoolday (green) of $\text{PM}_{2.5}$ concentration data. The potential exposure calculated using the primary SAMHE minutely $\text{PM}_{2.5}$ concentrations has contributions from every concentration bin up to and including $33 \mu\text{g}/\text{m}^3$. The potential exposure calculated using SAMHE hourly $\text{PM}_{2.5}$ concentrations leads to a similar distribution at concentration ranges below $15 \mu\text{g}/\text{m}^3$; however, for higher concentration ranges, the exposure calculated using SAMHE minutely $\text{PM}_{2.5}$ concentrations is not well represented by the exposure calculated using SAMHE hourly $\text{PM}_{2.5}$ concentrations. The potential exposure calculated using SAMHE schoolday mean $\text{PM}_{2.5}$ concentrations shows that the distribution is less well represented still. As such, we regard it as necessary to use high resolution $\text{PM}_{2.5}$ concentration data, ideally minutely, when making calculations to estimate the potential exposure.

	Continuous period data			School-year data		
	mean	standard deviation	median	mean	standard deviation	median
Primary SAMHE datasets	3.71	3.68	2.46	4.54	4.80	2.81
SAMHE datasets with hourly averaging	3.71	3.92	2.35	4.54	4.85	2.88
SAMHE datasets with minutely data	3.71	3.93	2.34	4.54	4.85	2.89
Alternate SAMHE datasets	3.62	3.64	2.41	4.39	4.68	2.71

Table C.1: Table comparing summary statistics of differing datasets; the mean, standard deviation and median are presented for the continuous period datasets, and for the SAMHE schoolday datasets, in each case. The first row shows statistics for the primary datasets reported herein, the second row statistics from datasets constructed with hourly-averaged datasets, the third row shows statistics from datasets constructed with minutely data, and the bottom row shows statistics from the datasets constructed using the alternate data completeness criterion.

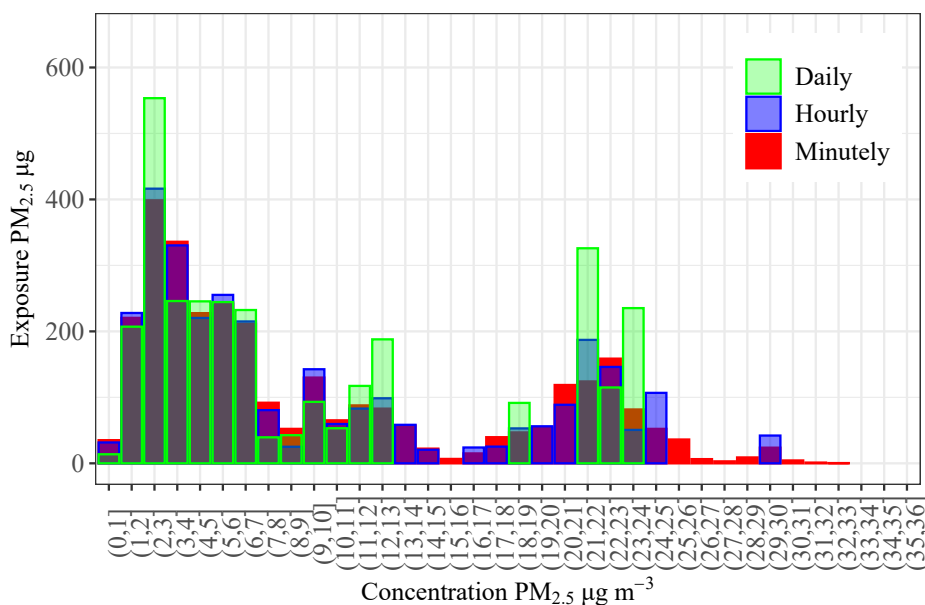


Figure C.3: The contribution to the total exposure during the school-year due to PM_{2.5} concentrations apportioned in to 1 µg/m³ bins. The exposure calculated from SAMHE minutely PM_{2.5} concentrations, as presented in §3.3 is shown in red, and in blue and green are the exposures calculated using the SAMHE hourly mean and SAMHE schoolday mean PM_{2.5} concentrations, respectively.

Appendix D. Evaluation of data completeness criteria for selection of PM_{2.5} concentration data

The results in §3 report trends of the primary datasets; namely, the continuous datasets and the schoolday datasets. The data completeness criteria, as detailed in §2.2.1, specified that on each day, data would be selected from only schools that reported data for over 75% of: the 24-hour period, in the case of the continuous datasets, or the school day (09:00—16:00) for the schoolday dataset. To test the sensitivity of the results to the choice of this criteria, alternate datasets were created using alternate data completeness criteria. The alternate data completeness criteria specified that, in addition to the criteria of the primary datasets, data is only selected from schools that report adequate data on more than 75% of days within the entire school-year. Table C.1 shows the mean, standard deviation and median calculated across all 295 values of the SAMHE 24-hour mean PM_{2.5} concentrations in the continuous period datasets, and all 133 values of SAMHE schoolday mean PM_{2.5} concentrations in the schoolday datasets, formed by both the primary and alternate data completeness criterion. Over the entire continuous period, should the alternate criteria have been selected, the mean would have been 0.09 $\mu\text{g}/\text{m}^3$ (or 2.43%) lower than the primary dataset, the median would have been 0.05 $\mu\text{g}/\text{m}^3$ (2.03%) lower, and the standard deviation 0.04 $\mu\text{g}/\text{m}^3$ (or 1.09%) lower, than for the primary dataset. Likewise, for the SAMHE schoolday data the mean would have been 0.19 $\mu\text{g}/\text{m}^3$ (or 4.1%) lower, and would the median and the standard deviation, by 0.07 $\mu\text{g}/\text{m}^3$ (2.52%) and 0.13 $\mu\text{g}/\text{m}^3$ (2.7%), respectively. To summarise, the choice of dataset construction between the primary datasets (in which included schools evolve throughout the year) and the alternate datasets (in which the population of included schools remains fixed throughout the year) does not result in significant differences in the reported results and does not affect any of the conclusions drawn.

Appendix E. Air-mass back trajectory analysis

Back trajectories were calculated using HYSPLIT (Hybrid Single Particle Lagrangian Integrated Trajectory) model, an atmospheric transport and dispersion model (see Stein et al., 2015, for full details). Gridded meteorological data (e.g. wind speed and direction, temperature, humidity, and precipitation) from the NCEP-NCAR Reanalysis meteorological model (Kistler et al., 2001) constitute inputs of the HYSPLIT model, which is run using the Openair R statistical software package (Carslaw and Ropkins, 2012). For an initial start location (longitude, latitude, and altitude) and time (the time that the air-mass arrives to the chosen location — herein London Honor Oak Park AURN site, see §3.2 for a discussion), the HYSPLIT model calculates the movement of a parcel of air due to the mean advection by wind using a Lagrangian method, iterating backwards in time at intervals of one hour for a duration of 96 hours (4 days) to calculate a given back trajectory. Back trajectories are presented based on air-masses arrival times, at the chosen location, every three-hours over the academic year. The trajectories of air-masses that arrive at the chosen location during PM_{2.5} events are compared to those that arrive at the chosen location at other times of the academic year, to determine if there are air-mass trajectories that are qualitatively different during PM_{2.5} events. Cluster analysis of trajectories was also conducted to objectively group trajectories based upon similarities in the paths they take. This analysis was conducted using the ‘trajCluster’ package within Openair, (Carslaw and Ropkins, 2012) which determines how similar two trajectories are by calculating the Euclidean distance between the 96 longitude and latitude coordinates along each trajectory (96 points for each 96 time iterations) using a Haversine formula.

Appendix F. Dates of outdoor PM_{2.5} events

In §3.2 the impact of periods of elevated AURN PM_{2.5} concentrations, or ‘PM_{2.5} events’, on the SAMHE PM_{2.5} concentration was investigated. Two definitions of PM_{2.5} events were evaluated. Namely, ‘WHO PM_{2.5} events’, which is any day, or consecutive days, for which the AURN 24-hour mean PM_{2.5} concentration exceeds 15 $\mu\text{g}/\text{m}^3$, and ‘Moderate PM_{2.5} events’ are defined as when the AURN 24-hour mean PM_{2.5} concentration exceeds 9.67 $\mu\text{g}/\text{m}^3$. The dates on which these events occurred, and their durations in days and schooldays, are summarised in tables F.1 and F.2, respectively.

Event	Start date	End date	Number of days	Number of schooldays
1	06/09/2023	10/09/2023	5	3
2	06/03/2024	11/03/2023	6	4
3	02/05/2024	02/05/2024	1	1
4	11/05/2024	12/05/2024	2	0

Table F.1: A complete list of the dates, and their durations in terms of days and schooldays, for the ‘WHO PM_{2.5} events’ analysed.

Event	Start date	End date	Number of days	Number of schooldays
1	05/09/2023	05/09/2023	1	1
2	16/09/2023	17/09/2023	2	0
3	09/10/2023	10/10/2023	2	2
4	12/11/2023	12/11/2023	1	0
5	16/11/2023	16/11/2023	1	1
6	25/11/2023	26/11/2023	2	0
7	29/11/2023	29/11/2023	1	1
8	01/12/2024	03/12/2024	3	1
9	06/12/2024	06/12/2024	1	1
10	13/01/2024	13/01/2024	1	0
11	24/01/2024	24/01/2024	1	1
12	29/01/2024	29/01/2024	1	1
13	31/03/2024	31/03/2024	1	0
14	01/05/2024	01/05/2024	1	1
15	06/01/2024	10/01/2024	5	0
16	13/05/2024	13/05/2024	1	0
17	18/05/2024	20/05/2024	3	0

Table F.2: A complete list of the dates, and their durations in terms of days and schooldays, for the ‘moderate outdoor PM_{2.5} events’ analysed.

Site	Plantower PMS5003 sensors (n)	Reference sensor	Test duration (days)	Observations (n)	RMSE ($\mu\text{g}/\text{m}^3$)	MAE ($\mu\text{g}/\text{m}^3$)
London Marylebone Road AURN	4	Met One BAM	336	752	2.25	1.87
London Honor Oak Park AURN	4	Palas Fidas 200E	336	816	2.72	2.19
University of Cambridge	6	Palas Fidas 200S	371	1302	2.31	1.79
Manchester	6	QuantAQ MODULAIR	64	384	2.65	1.52
Aggregated ‘co-located dataset’ analysed	20	As above	See above	3254	2.45	1.87

Table G.1: Summary of co-location tests and respective root mean square errors (RMSE) and mean absolute errors (MAE) between measurements of daily mean concentration made by reference sensors and Plantower PMS5003 sensors.

Appendix G. Co-located tests and the resulting datasets

Co-location tests using the Plantower PMS5003 sensors, within the AirGradient One monitors used by SAMHE, have been carried out at four different sites around the UK (AirGradient, 2024). In three of those all monitors were exposed to outdoor air, whilst in the fourth the monitors were all placed indoors. The three outdoor test sites consisted of the London Marylebone Road AURN site (there employing a Met One BAM sensor) and the London Honor Oak Park AURN site (employing a Palas Fidas 200E) — at each of which, four Plantower PMS5003 sensors were co-located — and a further site at the University of Cambridge (there also a Palas Fidas 200S sensor) — at which six PMS5003 sensors were co-located. At the fourth site, in Manchester, six Plantower PMS5003 sensors were co-located indoors with a QuantAQ MODULAIR monitor. Whilst we note this was not a reference grade monitor, separate co-location tests of a MODULAIR monitor co-located with regulatory-grade instruments has shown low mean absolute errors (MAE = $1.3 \mu\text{g}/\text{m}^3$) and high correlation coefficients ($R^2 = 0.936$) between the datasets, (Inc, 2023). To align with the analysis presented herein, we choose to analyse the daily mean concentrations recorded by all of the monitors included within the four co-location tests, these consisted of measurements over periods of 336, 336, 371 and 64 days, respectively. Given the numbers of low-cost sensors deployed, this corresponds to total observations of the daily mean concentrations measured by the Plantower PMS5003 sensors of 1208, 1168, 2160, and 384, at each of the four sites respectively.

The three outdoor sites consist of one site in London recording data officially described as representative of ‘urban traffic’ and two which can be regarded as urban background. Examination of the daily means from these three sites identified a presence of relatively high $\text{PM}_{2.5}$ concentrations at frequency not representative of the measurements of the indoor co-location tests nor the measurements of the SAMHE monitors, whilst also including a wealth of valuable data at more moderate $\text{PM}_{2.5}$ concentrations which does warrant inclusion. As such, from within the SAMHE dataset we identified the 95% percentile within the values of daily mean $\text{PM}_{2.5}$ concentrations measured, corresponding to a value of $13.3 \mu\text{g}/\text{m}^3$, and took this value as an upper threshold for inclusion of the co-located data gathered outdoor at outdoor sites. Outdoor co-location data was then included from any site on any days for which the average of all of the daily mean concentrations measured by the Plantower PMS5003 sensors at that site fell below the upper co-location threshold value. As such, the outdoor co-location data analysed herein better reflected the distribution of concentrations measured by both the indoor co-location data and by the SAMHE monitors. We note that the indoor co-location data included observations of daily mean $\text{PM}_{2.5}$ concentration as high as approximately $30 \mu\text{g}/\text{m}^3$, and hence the co-location data on which we report results does still include observations at the upper end of the measurements recorded by the SAMHE monitors. As a result, the co-location datasets finally analysed consisted of 808, 896, 1542, and 384 independent observations of the daily mean concentration, at each of

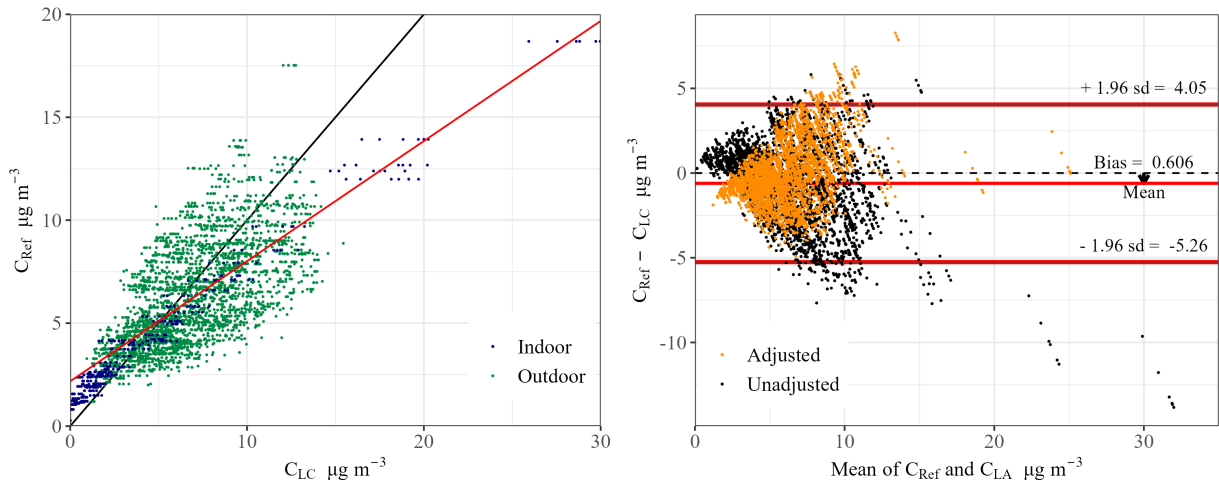


Figure G.1: The left-hand pane presents a scatter plots of the observations of daily mean concentrations in the co-location dataset, and the measurements by reference sensors (C_{Ref}) to those by low-cost Plantower PMS5003 sensors (C_{LC}). The colour of the circular markers denotes whether the co-location tests occurred indoors or outdoors. The black line shows the line of equality, and red line shows the least-squares fit to all data points (see text for details). The right-hand pane shows a Bland-Altman plot showing the difference between measurements by reference sensors and low-cost Plantower PMS5003 sensors ($C_{Ref} - C_{LC}$) against the mean of the two measurements ($(C_{Ref} + C_{LC})/2$). The black markers show all data analysed from the co-location tests. Horizontal red lines show the mean difference and limits of agreement (mean ± 1.96 standard deviations) of the data (marked in black), the width of the lines corresponding to the 95% confidence interval of each. Superimposed are the orange markers which show the data resulting from a Bland-Altman analysis with the low-cost co-located sensor data adjusted by the linear mapping from the least-squares fit shown in the left-hand pane — this same mapping is utilised to create the co-located data ‘adjusted SAMHE dataset’, as described in §Appendix G.

the four sites respectively. Table G.1 presents a summary of the resulting co-location datasets.

The daily mean concentrations measured by the reference sensors is plotted against those measured by low-cost Plantower PMS5003 sensors of the included aggregated observations in the left-hand pane of figure G.1. There is a strong correlation between the reference and low-cost measurements (with a Spearman’s rank correlation coefficient of approximately 0.74, with a p-value of $p < 2.2 \times 10^{-16}$). We note that when the measurements of 24-hour mean $PM_{2.5}$ concentration measured by Plantower PMS5003 sensors in SAMHE monitors are compared to the measurements made in reference grade AURN sites; there too, a strong correlation exists (the Spearman’s rank correlation is approximately 0.83, with a p-value of $p < 2.2 \times 10^{-16}$), see §3. Conducting a Bland-Altman analysis (Giavarina, 2015) of the aggregated co-location dataset reveals that there is a mean bias of $-0.61 \mu\text{g}/\text{m}^3$ of Plantower PMS5003 measurements relative to the reference measurements — indicating that the concentrations recorded by the Plantower PMS5003 sensor, on average, slightly exceed those of the co-located higher grade sensors (we note that the bias systematically varies with concentration becoming positive for concentrations less than approximately $4 \mu\text{g}/\text{m}^3$, see right-hand pane of figure G.1). As such, the potential for this bias (expected within the measurements made by the Plantower PMS5003 $PM_{2.5}$ sensors within the SAMHE monitors based on the co-located data) to impact our findings are quantified in Appendix H by analysing datasets adjusted with the intent to account for this bias.

Lastly, as a point of reassurance and fact, it is expected that the low-cost sensors will produce measurements containing greater levels of random noise than the reference sensors. The daily mean concentrations measured by the Plantower PMS5003 sensors and by reference sensors are not normally distributed (Kolmogorov-Smirnov test statistics 0.91 with a p-value $p < 2.2 \times 10^{-16}$ and 0.95 with a p-value $p < 2.2 \times 10^{-16}$ for the two distributions respectively). As such, a Levene’s test was used to reveal that the larger variance within measurements of the daily mean concentrations measured by the Plantower PMS5003 sensors, relative to that measured by reference sensors, was indeed significant ($F(1, 6506) = 97.05$, with a p-value $p < 2.2 \times 10^{-16}$).

	Continuous period data			School-year data		
	mean	standard deviation	median	mean	standard deviation	median
Primary SAMHE datasets	3.71	3.68	2.46	4.54	4.80	2.81
Co-located data ‘adjusted SAMHE datasets’	4.34	2.17	3.60	4.82	2.83	3.81

Table H.1: Table comprising of the summary statistics for the primary SAMHE dataset reported throughout §3 and of the ‘adjusted SAMHE dataset’ created by applying a linear mapping based upon the aggregated included co-location dataset, described in §Appendix G.

Appendix H. Analysis of the adjusted SAMHE datasets

Applying a linear, least squares, fit to the daily mean concentrations measured by the low-cost PMS5003 sensor, C_{LC} , and the corresponding measurements from the co-located reference sensors, C_{Ref} , revealed the relationship: $C_{Ref} = 0.59C_{LC} + 2.15$ (with a coefficient of determination, $R^2 = 0.58$) indicates, in agreement with the Bland-Altman analysis (see Appendix G), the potential for bias in the data. Overlaid within the Bland-Altman plot (right-hand pane of figure G.1) are orange markers indicating the co-located low-cost measurements after being subjected to a mapping according to this linear relationship. The bias of this adjusted co-located dataset is negative at both low and moderate concentrations, indicating that adjusted low-cost measurements could be expected to exceed those of reference grade sensors. ‘Adjusted SAMHE datasets’ were created by applying the same linear mapping to the measurements of $PM_{2.5}$ within the primary SAMHE datasets.

Finally, we now quantitatively report any impact on our results, of §3), when instead analysing the adjusted SAMHE datasets. The statistics of the adjusted SAMHE dataset (summarised in table H.1) exhibit increases, relative to the primary dataset, in the mean concentrations for the continuous period data, by $0.63 \mu\text{g}/\text{m}^3$, and by $0.28 \mu\text{g}/\text{m}^3$ for the school-year. The correlation coefficients reported for the AURN and SAMHE $PM_{2.5}$ concentrations remain identical and, as would also be expected, the indoor-outdoor ratios are slightly increased, on average, when analysing the adjusted dataset. In §3.1, by comparing the difference between mean of SAMHE and AURN $PM_{2.5}$ concentrations over the school-year and continuous period we ascertained that sources $PM_{2.5}$ generated within school buildings could be responsible for up to 25% of the $PM_{2.5}$ concentrations, applying the same argument to the adjusted SAMHE dataset this upper bound would be decreased to 16%. The estimate of the total potential exposure over the academic year is slightly increased when the adjusted SAMHE dataset is analysed, providing an estimate of $3234 \mu\text{g}$ compared to the value of $3014 \mu\text{g}$ (3), and we note that the distribution of the exposure in $1 \mu\text{g}/\text{m}^3$ bins (e.g. figure 4) is marginally altered, shifting the distribution to slightly lower concentrations. The proportion of the exposure received during $PM_{2.5}$ events decreased, contributing to 29% of the total exposure, of which, 18% is received during WHO $PM_{2.5}$ events and 11% during Moderate $PM_{2.5}$ events (with the corresponding figures from the unadjusted SAMHE dataset being 41%, 27%, and 14%, respectively). In short, applying a calibration to the SAMHE dataset based upon co-location data has only minor impacts on some of the quantitative results obtained and no impact on the conclusions drawn.